Charles University

Faculty of Medicine in Hradec Králové

DISSERTATION THESIS

Jan Večeřa, M.D. **2020**

Charles University
Faculty of Medicine in Hradec Králové

Doctoral Study Programme

Internal Medicine

The Utility of Three-dimensional (3D) Colour Doppler Echocardiography for the Evaluation of Dynamic Changes of Secondary Mitral Regurgitation during Dynamic Stress Echocardiography

Možnosti Využití Trojrozměrné (3D) Echokardiografie při Měření Dynamických Změn Funkční Mitrální Insuficience při Zátěžové Echokardiografii

Jan Večeřa, M.D.

Supervisor: Associated Professor Radovan Malý, M.D., PhD.

Hradec Králové, 2020 Defence on: .....

Author‘s Declaration

Declaration:

I declare hereby that this dissertation thesis is my own original work and that I indicated by references all used information sources. I also agree with depositing my dissertation in the Medical Library of the Charles University, Faculty of Medicine in Hradec Králové and with making use of it for study and educational purpose provided that anyone who will use it for his/her publication or lectures is obliged to refer to or cite my work properly.

I give my consent to availibility of my dissertation’s electronic version in the information system of the Charles University.

Hradec Králové, 2020

Signature of the author

Acknowledgements

I wish to express my gratitude to my supervisors: Associated Professor Radovan Malý and Professor Jan Bureš who gave my full support and guidance during my studies and who were extremely tolerant even though my studies were prolonged.

The whole concept of my work has been set up during my fellowship in Echocardiographic laboratory in Cardiovascular Centre Aalst, Belgium under the supervision and guidance of Associated Professor Martin Pěnička, who has taught me almost everything about scientific work, cardiac imaging and changed (or established) my way of thinking as concerns the science, collaboration, humbleness and especially about the way how the mentor should treat his student.

I would like to thank to the head of our internal clinic in Pardubice Dr. Petr Vojtíšek and Dr. Jan Matějka together with Dr. Aleš Havlíček who all supported me in 2011 to leave our institution for the Fellowship in Belgium and who kept my job for the whole time of my exile. For the statistical analysis I would like to thank to RNDr. Marek Malý, CSc.

I would also like to thank to my colleague Dr. Martin Kotrč my co-fellow in Aalst, a very good friend and a great support for the period of our fellowship.

Finally, I wish to thank to my wife Jana and my daughters Ema and Barbora who make my life and work worth living.

Abbreviations used

2D – two-dimensional

3D – three-dimensional

3DE – three-dimensional echocardiography

CABG – coronary artery bypass

CRT – cardiac resynchronisation therapy

CMR – cardiac magnetic resonance

CW – continuous wave Doppler

EROA – effective regurgitant orifice area

FMR – secondary/functional mitral regurgitation

LA – left atrium

LV – left ventricle

LVOT – left ventricle outflow tract

MI – myocardial infarction

MR – mitral regurgitation

PISA – proximal isovelocity surface area

PLAX – parasternal long axis

PW – pulsed wave Doppler

RVol – Regurgitant volume

TEE – transesophageal echocardiography

TTE – transthoracic echocardiography

VC – vena contracta

VCA – vena contracta area

VTI – velocity time integral of the flow

Table of contents

Introduction

Our study originated from the fusion of two distinct methods for the evaluation of patients with secondary-functional mitral regurgitation (FMR). The first one – dynamic stress echocardiography is currently not frequently used due to limited human and time resources and the second one: three-dimensional echocardiography is rather on its way, to be established in echocardiographic laboratories for the clinical routine use. By fusion of both methods we wanted to seek for new ways of evaluation of functional mitral regurgitation.

Therefore, following paragraphs briefly review current knowledge on the problematic of secondary – functional mitral regurgitation and its dynamic behaviour during stress dynamic echocardiography, standard techniques for the mitral valve regurgitation quantification and three-dimensional echocardiography methods.

1.1. Mitral Valve Regurgitation

Mitral valve regurgitation (MR) is a common and progressive condition that is difficult to manage clinically.[1, 2]MR results from several heterogeneous conditions, including disorders of the mitral valve leaflets, mitral annulus, chordae tendinae, papillary muscles, and the ventricle. [3]In contrast to the primary , also called degenerative MR, where the valve itself is diseased, secondary MR results from the geometrical distortion of the subvalvular apparatus, which occurs secondary to LV enlargement and impaired contractility. [3-5] Secondary MR (also functional) is a disease of the ventricle rather than of the valve and in Carpentier ´s surgical classification if mitral valve pathology belongs to the type IIIb. [6].

FMR is a challenging problem in terms of diagnostic and therapeutic implications in heart failure patients. It occurs in 11% to 59% of patients after myocardial infarction [7, 8]and is present in more than 50% of patients with dilated cardiomyopathy.[9, 10]The presence of even mild SMR is a marker of more advanced disease and it is associated with poor outcome of the patient regardless of the left ventricle systolic function.

Mitral regurgitation has also dynamic behaviour during exercise or with changing loading conditions. Presence of mild mitral regurgitation at rest is sometimes discordant with the

patient´s complaints of dyspnoea on effort and only exercise stress testing may reveal significant dynamic increase of MR severity. Such dynamic behaviour of the MR was described in primary MR [11, 12] and more profoundly in secondary MR as described in deep further in text.

Figure 1: Interplay between tethering and closing forces. Functional-secondary mitral regurgitation (Carpentier type IIIb) is a valvular dysfunction secondary to a myocardial disease. An imbalance between closing and tethering forces inhibiting normal mitral leaflet coaptation is the underlying mechanism of the disorder. (adapted from Dr.Penicka with permission)

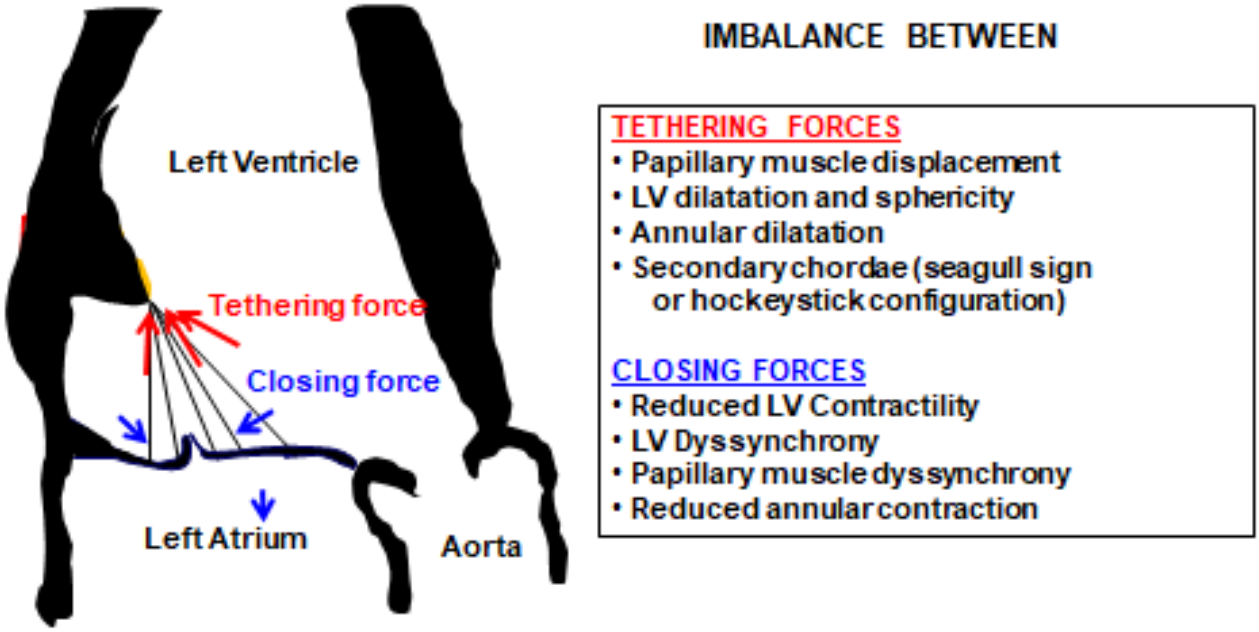

1.2. Pathophysiology of secondary mitral valve regurgitation

The mitral valve apparatus is a complex apparatus comprised of multiple components such as the mitral annulus, anterior and posterior leaflet, chordae tendinae, anterolateral and posteromedial papillary muscles, and adjacent left ventricular wall. All these structures are tuned to work together in sealing the passage of the blood from the left ventricle to the left atrium in systole while enabling unrestricted inflow during diastole. Several mechanisms play

role during systole: annular contraction, left ventricular wall motion causing inward displacement of the papillary muscles to facilitate leaflet coaptation, and finally contraction of the papillary muscles to avoid leaflet prolapse. As depicted in Figure 1 a balance is maintained between tethering forces represented by left ventricle wall, papillary muscles, chordae tendinae and closing forces represented by left ventricular contractility, synchrony and mitral annular contraction. Malfunction of any of these structures may lead to mitral regurgitation.[13]

The dysbalance of closing and tethering forces is dynamic throughout the one cardiac cycle. The typical behaviour of the secondary MR is represented by decrease of its severity in mid-systole during ventricular contraction at the time of peak orifice velocity and peak systolic pressure. This suggests important impact of ventricular-to-atrial pressure difference on leaflet coaptation, where mid-systolic decrease of annular area plays limited role as described previously. [14, 15] However, closing forces represented very well by dP/dt do not play the most important role in in secondary MR. It is proven that tethering forces are prerequisite for the secondary MR. Typical example of tethering forces leading to mitral valve leaflet restriction shows Figure 2. [16-18] Finally , also geometric disturbances of the left ventricle with papillary muscles position and dynamics are the major determinants in the pathophysiology of the FMR. [19, 20] Interestingly, in patients with long persistent atrial fibrillation isolated mitral annulus dilatation was described leading to more than moderate MR even in patient with normal left ventricular dimensions and function and in this population rhythm control with ablation strategies or annular reduction may lead to improvement. [21, 22]Recently, active leaflet growth was described in patient as an adaptation to the mechanical stretch in patients with severe chamber dilatation reducing the impact of tethering forces and reducing the severity of FMR. [23, 24].

Figure 2: An example of a typical echocardiography appearance of the normal mitral valve (2A) and distorted mitral valve geometry leading to FMR (2B). In healthy individuals with a normal left ventricle (2A), mitral valve leaflets are "flat" with the coaptation point almost at the annulus plane. In contrast, in dilated LV with FMR (2B), the leaflets are pulled toward the LV apex due to the stretching of chordae, which results in so called tenting of the anterior leaflet and restrictive systolic motion of the posterior leaflet with the coaptation point displaced apically and posterolaterally. (adapted from Dr.Penicka with permission)

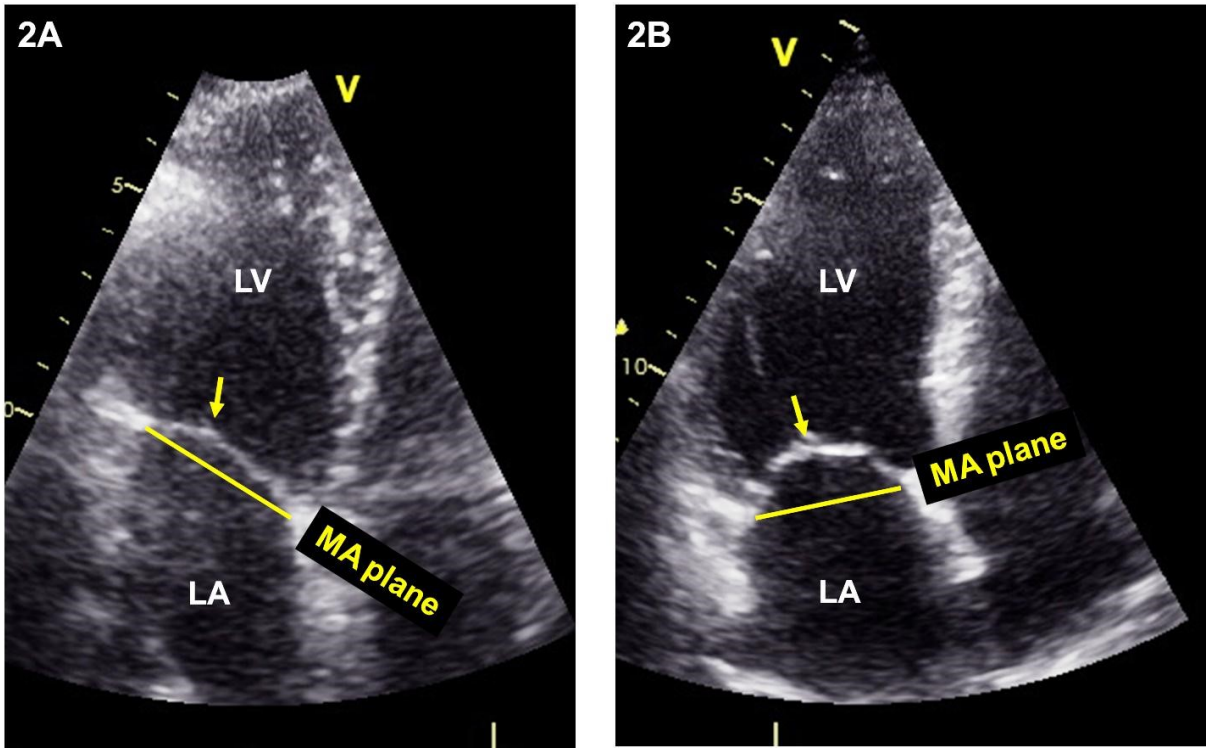

1.3. The Normal Cardiovascular Response to Exercise

The cardiovascular system adapts to meet increased oxygen demands of peripheral muscles during exercise. [25]Sympathetic system stimulation and the vagal tone drop result in increased heart rate and myocardial contractility, decrease in systemic vascular resistance thus increasing cardiac output. [26]In dynamic exercises where multiple muscle groups contract to achieve locomotion through the joint movement, we observe profound vasodilatation in the muscular vasculature, causing a significant reduction in systemic vascular resistance to half of its value at rest and corresponding increased venous return due to skeletal muscle pump. The rise in cardiac output is mediated through the increase in

stroke volume (due to increased contractility, decreased afterload and increased venous return) together with heart rate increase, which becomes important when stroke volume reaches its plateau. In static exercise, systemic vascular resistance remains the same or even rises and therefore cardiac output depends only on the heart rate. Static exercise is a model pressure load on the left ventricle whereas dynamic exercise imposes a volume load. Such pressure or volume loading conditions translate into different left ventricular geometric changes during exercise as studied with radionuclide angiography[27], echocardiography [28, 29]or cardiac magnetic imaging.[30] In healthy individuals we observe no or minimal increase in left ventricular (LV) end-diastolic volume and concomitant decrease in LV end-systolic volume leading in stroke volume and ejection fraction increase. In static exercise we do not observe such changes. [31]Substantial increase in cardiac output during exercise imposes huge load impact on pulmonary circulation with the slight impact with slight increase in left atrial pressure. Pulmonary circulation recruits and distends pulmonary arterial vessels, hence decreasing the pulmonary vascular resistance. In healthy individuals the increase of mean pulmonary artery pressure does not cross 3.0 mmHg/L/min but the role of age plays significant role.[32, 33] Mean pulmonary artery pressure during exercise with cardiac output ≤ 10L/min should not exceed ≥ 30mmHg, however, in trained athletes, values above 50mmHg have been observed. [34]

1.4. Exercise echocardiography protocol concept

A comprehensive resting echocardiogram is crucial in identifying the mechanism of MR, its severity, left ventricle systolic function and regional wall motion, diastolic function and calculate estimated pulmonary artery pressure gradient. LV ejection fraction and LV volumes are calculated using Simpson's biplane method. The severity of MR should be quantified by calculating the effective regurgitant orifice (ERO) area using proximal isovelocity surface area (PISA) method, which is well established as a golden standard for the MR´s severity quantification and which could be measured in more than 90% of the patient during exercise. [3, 35]. In case when it is not possible to reliably use the PISA method, especially in MR with extremely eccentric jets, other method such as 2D derived vena contracta width measurement should be used. Average of 3 cycles should be used.

The most appropriate way of mitral valve stress testing is performed using a semi-supine exercise bicycle (Figure 0, page 53) with an increase in workload every 2 minutes until

symptoms develop or the patient can´t continue because of fatigue or any other reason for the test termination occurs. Continuous blood pressure, heart rate, electrocardiography and oxygen blood saturation monitoring is mandatory. It is possible to use the treadmill and perform post-exercise measurements, but these may not represent the true peak hemodynamics and we may miss the most important information.

Dobutamine SE is of limited role in the assessment of dynamic MR. It does not allow evaluation of functional capacity. Furthermore, the hemodynamic changes induced by dobutamine infusion are different to those that we observe during exercise. In patients with heart failure, dobutamine generally improves cardiac output and stroke volume and it is associated with the reduction in the severity of MR where conversely exercise may increase MR severity and reduce stroke volume. [36, 37].

1.5. Secondary Mitral Regurgitation during Exercise

The response of the left ventricle to the dynamic or static exercise is different in patients with ischemic or dilated cardiomyopathy compared to the normal subjects. Pressure loading in the static exercise led to left ventricular dilatation with preserved ejection fraction and a drop in forward stroke volume with MR rise, all attributable to the significant rise in afterload hardly counterweighted by closing force increase. During dynamic exercise significant increase in end-diastolic and end-systolic volume was observed, much more profound in ischemic cardiomyopathy, probably related to the extent of the myocardial scar. [38-41]In general, increased volume load together with inadequate arterial dilatation during exercise leads to left ventricular dilatation.

Several studies in ischemic and non-ischemic cardiomyopathy demonstrated the increase in secondary MR in more than 75% of patients. Table 1a,b (adapted from Bertrand et al., 2017) summarizes the current literature on determinants. Surprisingly, at rest, there were no significant determinant of dynamic MR including neither LV ejection fraction nor LV end-diastolic volume and with others variables in contradictory results. In our study, we observed the same lack of predictors of dynamic MR at rest. On the contrary, as documented in table 1b exercise-induced changes in LV shape and sphericity correlates very has profound effect on mitral geometry. Papillary muscles dyssynchrony plays also the significant role. Dysbalance between closing and tethering forces during exercise could be also observed

very well in tenting area rise. Annular dilatation progression in exercise is significant predictor of dynamic MR in patients with dilated cardiomyopathy. [42-48]

The impact of left ventricular scar in ischemic cardiomyopathy was proven is also related to the localisation of the scar. Patients with anterior wall myocardial infarction (MI) extending to the apical region of inferior wall have apically tethered mitral leaflets, with coaptation depth being determinant of exercise-induced dynamic MR. [43, 49] In patients with inferior wall infarction, we observe during exercise mitral valve leaflets tethered more posteriorly, especially posterior mitral leaflet and increasing the annular dimension (around P2-P3) increasing MR. On the contrary, if contractile reserve of the inferoposterior wall is present, the exercise-induced decrease in MR is present due to reduced tethering forces and preserved mitral annulus distortion. [45]Large or multiple infarctions which induce severe remodelling leading to more spherical ventricles with pronounced papillary muscle separation exerting traction on the mitral valve from opposing ends. The differential left ventricular response to exercise in cardiomyopathy based on the underlying aetiology and location of the scar is shown in Figure 3.

Figure 3. The differential left ventricular response to exercise in cardiomyopathy based on the underlying aetiology and location of the scar. Determinants of worsening secondary MR during exercise are highlighted for each situation. (Adapted from Bertrand et al., with permission)[50]

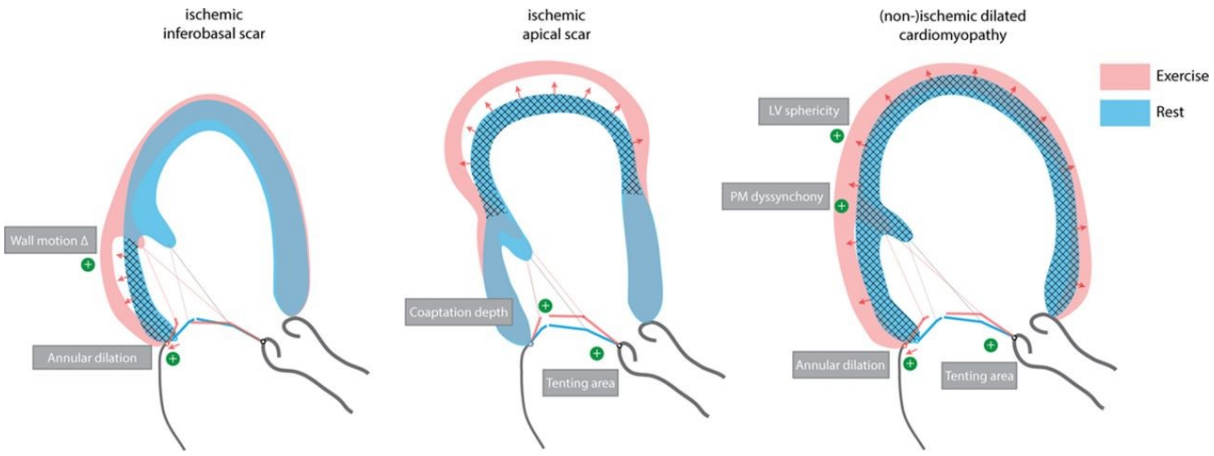

Anyone who has ever witnessed acute myocardial ischemia during dynamic exercise echocardiography revealing reversible myocardial wall motion abnormalities will never forget if dynamic exercise induced MR was induced. This type of dynamic secondary MR associated with reversible wall motion abnormalities is an excellent target for myocardial revascularization and completely reversible when revascularized. However, the term ischemic mitral regurgitation is not reserved for such type of dynamic MR, but it is reserved for the patients with dynamic MR due to scar tissue and left ventricular remodelling who suffered from myocardial infarction. [51, 52]

The battle between closing and tethering forces during exercise. As listed in Table 1a and 1b, the predictors of increasing secondary MR during exercise are related to the left ventricular geometry. {Bertrand, 2017 #72}

Table 1 a): Geometric determinants of increasing secondary mitral valve regurgitation during exercise AT REST

Author	N	IMR	Regression	LVEDD	LVEF	LV Sphericity	LV Dyssynchrony	Annular dilatation	Tenting Area	Coaptation Depth	WMSI
Giga et al., 2005	40	100%	UV, MV	-	-	-		-	-	-	-
Ennezat et al., 2006	70	50%	UV MV	+ -	- -		+ +				
Takano et al., 2006	17	29%	UV		-						
Yamano et al., 2008	32	0%	UV	-	-	+		-	+	-	
Izumo et al., 2009	50	32%	UV MV	-	-	+		-	-	-	

Table 1 b): Geometric determinants of increasing secondary mitral valve regurgitation during exercise CHANGES DURING EXERCISE (Adapted form Bertrand et al., 2017, with permission)

Author	N	IMR	Regression	LVEDD	LVEF	LV Sphericity	LV Dyssynchrony	Annular dilatation	Tenting Area	Coaptation Depth	WMSI
Keren et al., 1989	17	50%	UV	-							
Lapu-Bula et al., 2002	25	50%	UV	-		+		-		-	
Lancellotti et al., 2003	70	100%	UV MV	-	-			+	+	+	+
Giga et al., 2005	40	100%	UV MV	-	-	+		+ -	+ +	+ +	+ -
Lancellotti et al., 2005	35	100%	UV MV	-	-		+ +		+ +		
Ennezat et al., 2006	70	50%	UV MV					+ +			
D´Andrea et al., 2007	60	0%	UV MV	-	-		+ +		+ +		
Yamano et al., 2008	32	0%	UV	-	-	-		-	+	+	
Izumo et al., 2009	50	32%	UV MV	-	-	+ +	+ +	+ -	+ -	+ +	

The symbol + indicates the association between geometric determinant (and change in the determinant) and the severity of secondary MR during exercise (in univariate (UV) or multivariate (MV) analysis). The symbol – means no correlation. All studies were free of inducible ischemia. IMR, ischemic mitral regurgitation; LV, left ventricle; LVEDD, left ventricle end-diastolic dimension; LVEF, left ventricular ejection fraction; WMSI, wall motion score index.

Therefore we may conclude, that increase in tethering forces on the mitral valve leaflets by far outweighs increase in closing forces. Cardiac resynchronisation therapy (CRT) brings an excellent insight in the pathophysiology of the secondary MR. Madaric et al. , in their impressive study, proved that early after CRT we observe significant drop in secondary mitral valve severity within one week after CRT, but there was no effect on the dynamic MR during exercise. Significant decrease in dynamic MR was observed after 3 month follow up when left ventricle remodelled. CRT is associated with acute decrease in resting MR but does not immediately attenuate exercise-induced MR. In contrast, only late, CRT-induced reversed LV remodelling and reduced mitral apparatus deformation are associated with a reduction in both resting and exercise-induced MR and with an improvement in cardiopulmonary performance. [53] Typical example of the patient responding well to the CRT and FMR behaviour at rest and during exercise is presented in Figure 4.

Figure 4 Impact of cardiac resynchronisation therapy on secondary mitral valve regurgitation during exercise.

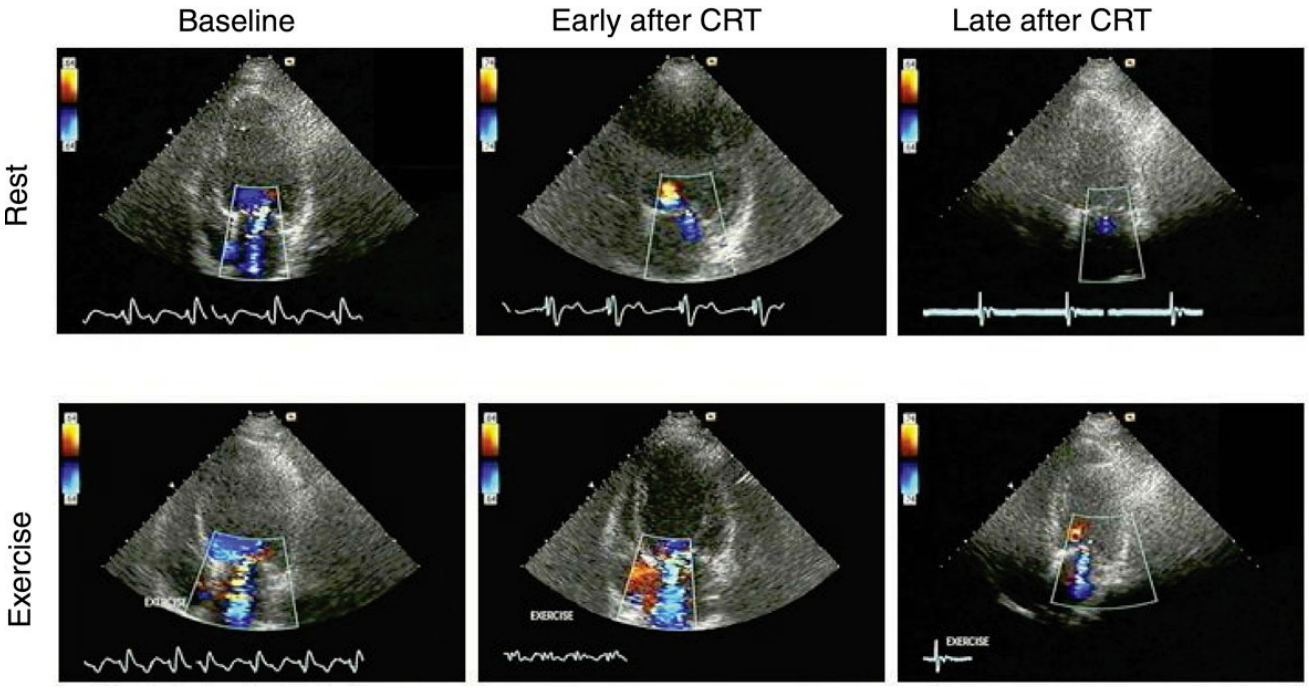

Early after CRT implantation, there is a significant drop in MR severity at rest. In contrast during exercise, there is no difference early after CRT, with significant dynamic MR. After 3 months with CRT when reverse remodelling of the left ventricle has occurred there is a significant reduction in exercise-induced MR. (adapted from Madaric et al., with permission (53))

1.6. Prognostic impact of dynamic mitral valve regurgitation

The exercise-induced increase in secondary MR is associated with poor exercise capacity and outcomes. [6, 47, 54-56] Lapu-Bula et al. were the first to demonstrate a significant negative impact of exercise-induced secondary mitral regurgitation on exercise capacity, although MR was only mild to moderate at rest. [47]Their excellent invasive study in Heart failure patients peak VO2, exercise-induced changes in stroke volume, and those in capillary wedge pressure correlated with the changes in MR (r=-0.55, -0.87, and 0.62, respectively, P<0.01). The changes in MR severity also correlated with those in end-diastolic (r=-0.75, P<0.01) and end-systolic (r=-0.72, P<0.01) sphericity indexes and those in the coaptation distance (r=0.86, P<0.01). Increased left atrial pressures, in patients with dynamic exercise-induced MR, cause

backward pulmonary venous congestion inducing pathological changes in the pulmonary vasculature, increasing pulmonary vascular resistance and pulmonary arterial pressure. As proven by further investigation systolic pulmonary arterial pressure during exercise correlates well with increase in effective regurgitant orifice area (ERO) and the level of dyspnoea [6, 57]and it is very useful echocardiographic parameter to assess during exercise as proven by Cleassesn et al. In invasively correlated study [58], for prognostication of secondary MR.

In another excellent study by Pierard and Lancellotti [59] a group of patients with the history of pulmonary oedema was matched and compared with the group that had no such history but comparable resting characteristics and all patients underwent exercise echocardiography. During exercise, regurgitant volume and the effective regurgitant orifice area increased (by 26±14 ml and 16±10 mm^2, respectively) in all but one patient with pulmonary oedema, where in contrast, small exercise-induced changes were observed in the comparison group. Furthermore, Lancellotti has proven in two landmark studies with reasonable follow up, that secondary mitral regurgitation in patients with ischemic cardiomyopathy is an independent predictor of mortality, hospital readmission rate in patients with MR with ERO ≥20mm2 and with dynamic ERO increase of ≥13mm2. [6, 49]

These values contrast to the cut-off value in primary –degenerative mitral valve regurgitation of ≥40mm2. The reason might be the underlying myocardial heart disease in secondary MR bearing prognostic issues and probably with an impact of dynamic nature of secondary MR – typically underestimated at rest. All the therapies should therefore probably aim at a dynamic component of secondary MR.

1.7. Treatment approaches for secondary mitral regurgitation

It is beyond the scope and purpose of our study to discuss the evidence of possible therapeutic approaches to the dynamic mitral valve regurgitation and current recommendation are represented by recent guidelines (Baumgartner et al, 2017) [60]. The most important issues related to this topic are listed accordingly:

1) Echocardiography is essential to establish the diagnosis of secondary mitral regurgitation.

2) All the recommendation regarding treatment of secondary mitral valve regurgitation remains controversial because, so far, no survival benefit has been found for the reduction of secondary mitral regurgitation.
3) It is unclear if the prognosis is independently affected by sole mitral regurgitation or whether it is mainly reflecting an impaired function of the left ventricle.
4) In case of isolated mitral valve regurgitation treatment the thresholds of the severity of mitral regurgitation for intervention still need to be validated in clinical trials.
5) In secondary mitral regurgitation, lower thresholds have been proposed to define severe mitral regurgitation compared with primary mitral regurgitation (20 mm2 for effective regurgitant orifice area (EROA) and 30 mL for regurgitant volume) owing to their association with prognosis. [61]
6) The severity of secondary mitral regurgitation should be reassessed after optimized medical treatment.
7) Secondary mitral regurgitation is a dynamic condition; echocardiographic quantification of mitral regurgitation during exercise may provide prognostic information of dynamic characteristics.
8) Myocardial viability testing may be useful in patients with ischemic secondary mitral regurgitation who are candidates for revascularization [60]

In brief, the potential impact of therapeutic approaches on the dynamic behaviour of secondary MR is listed below in Table 2 (modified from Bertrand et al., 2017){Bertrand, 2017 #72}

Table 2: The impact of current treatment approaches on geometric determinants of exercise-induced secondary MR, where + indicates impact on the determinant in terms of inhibition of its exercise-induced aggravation (adapted from Bertrand et al., 2017, with permission)

	LV sphericity	**PM dyssynchrony**	**Wall motion**	**Annular dilatation**	**Tenting area**
Medical therapy	**+**	**+/-**		**+**	**+**

Cardiac resynchronisation therapy	+	+	+	+	+
Revascularisation	+		+	+	+
Restrictive annuloplasty	+			+	+
Ventricular approach	+			+	+
Subvalvular approach					+
MitraClip	+			+	+

LV, left ventricle; PM, papillary muscles

1.7.1. Medical therapy

Medical therapy is a cornerstone of treatment of patients with chronic heart failure. The basic concept of neuro-humoral blockage is a golden standard, reversing adverse left ventricular remodelling. [62] Preload-reducing drugs such as diuretics or nitrates decrease tethering forces and EROA accordingly and also may enhance closing forces due to the left atrial pressure reduction. Afterload reducing drugs may relieve tethering forces by decreasing the left ventricular size and improving its shape. It remains controversial whether all these probable benefits would translate into exercise dynamics of the secondary MR.

1.7.2. Cardiac Resynchronisation therapy (CRT)

CRT reduces secondary MR and significantly reduces outcomes and quality of life in patients with heart failure and left ventricular systolic dysfunction together with intra-

ventricular conduction delay. [63]CRT reduces secondary MR and improves outcome in several ways in acute and chronic settings.

a) Acute effect of CRT results in dP/dT rise and longer duration and papillary muscles contraction synchronisation – therefore increasing closing resp. Reducing tethering forces. [64, 65]
b) Chronic effect of CRT is related to the long-term reverse left ventricular remodelling with left ventricle end-diastolic and end-systolic volume reduction – yielding the most clinically significant effect of the CRT.

As proven by Madaric et al. [53] the mechanism of CRT is associated with an acute decrease in resting MR but does not immediately attenuate exercise-induced MR. In contrast, only late, CRT-induced reversed LV remodelling and reduced mitral apparatus deformation are associated with a reduction in both resting and exercise-induced MR and with an improvement in cardiopulmonary performance. With CRT withdrawal within a short or long period (few days, 6 month), immediate increase in MR was observed. [66]

1.7.3. Revascularisation

Penicka et al. [67] in their prospective study proved secondary MR improvement at 1 year after isolated coronary artery bypass (CABG) in presence of ≥5 viable segments in the absence of papillary muscle dyssynchrony. In general, revascularization may improve viable myocardial segments and enhance left ventricle remodelling – which may reduce resting and even also a dynamic component of the secondary MR. When a contractile reserve is present during exercise, especially when inferior segments are involved, exercise MR is attenuated [43, 45] and papillary muscle dyssynchrony is independent determinant of exercise-induced MR.

When reversed, we may postulate that in patients with absence of myocardial viability and/or papillary muscle dyssynchrony, undergoing isolated CABG, are not likely to show improvement in their secondary MR and other adjunctive therapies should be taken in account.

Fattouch et al. [68] in their prospective randomized study compared CABG vs. CABG with mitral valve annuloplasty using postoperative exercise echocardiography and proved that the dynamic component of MR remained highly prevalent in CABG group but not in CABG with annuloplasty group. Improvement in exercise capacity with CABG and mitral valve annuloplasty after 1 year compared with isolated CABG was observed in RIME trail .[69] In contrast, the Cardio Thoracic Surgical Trails Network (CTSN) no different in clinical outcome, functional capacity or left ventricular remodelling was observed in 1 year of follow-up in 301 patients with moderate ischemic MR , receiving CABG or CABG with mitral valve annuloplasty. [70]

1.7.4. Mitral Valve Surgery

It is difficult to make any fundamental recommendations for the secondary MR especially in case of moderate secondary MR with a dynamic component. Preoperative exercise echocardiography was done only in RIME trial. It is unclear whether we should use some alternative cut off values for the MR severity. The former European Society Guidelines suggest mitral valve intervention in dynamic MR when there is concomitantly other reason for cardiac surgery (such as CABG) [2]

Different strategies for the mitral valve surgery were evolved and mitral valve annuloplasty, ventricular and subvalvular approaches or with mitral valve replacement are used, but the best strategy must be tailored according to the local expertise. However, it seems to be proven, that the size of the orifice remaining for the diastolic flow through the new or remodelled valve plays crucial role for the functional capacity, exercise-induced pulmonary hypertension and even for the prognosis of the patients! [71, 72]

1.7.5. Transcatheter Mitral Valve Interventions

The MitraClip device (Abbot Vascular) is based on principles of Alfieri stitch – the relatively simple surgical technique used primarily for the organic primary mitral valve regurgitation where a stitch is placed to seal the edges of the mitral valve together. The MitraClip device is a clip, deployable through the trans-septal puncture via left atrium percutaneously clipping the leaflets together. MitraClip acutely increases coaptation area

and slightly decreases antero-posterior annular dimension. In patients where reverse left ventricle remodelling was observed the tenting area also decreases. [73]

2. Mitral Valve Regurgitation quantification, the current recommendation

Echocardiography plays a key role in the assessment and management of the patients with mitral valve regurgitation.

The very first step for the evaluation is the comprehensive assessment of the mitral valve anatomy and function. According to the aetiology the MR is classified as a primary (organic, degenerative, structural) or secondary (a valve without significant structural abnormalities).

Our interest is focused on the secondary MR, which develops in patients with ischemic heart disease, dilated cardiomyopathy or in case of severe atrial dilatation.

2.1. Echocardiographic evaluation of the MR severity

There are three possible techniques for the MR severity assessment with colour Doppler imaging modalities, which is a primary screening modality for MR.

2.1.1. Colour flow Doppler

Colour flow imaging is the most common way to asses MR severity. We assume that the size and the extent of the jet into the left atrium (LA) increases with the severity of the MR. Hence, small thin jets just beyond the mitral valve leaflets represent smaller MR than large colour jets spreading to the depth of the LA. However, there are several technical and haemodynamic factors causing that the relationship between the size of the jet and MR severity is rather weak. Typically in patients with eccentric jets or with high LA pressures or low blood pressure could be easily underestimated in contrast to MR with central jets, normal LA pressures and/or higher left ventricle afterload. Individual example of the pitfall related to colour flow Doppler MR is presented in Figure 5. [74]

Is it quite a frequent mistake among junior echocardiographer to assess the severity of MR by eyeballing of the colour flow area, however, we may conclude that a small non-eccentric jet with a narrow vena contracta (VC≤3mm) and no visible flow convergence represents mild MR. And on the contrary, a large eccentric jet adhering, swirling and reaching the posterior wall of the LA is in favour of severe MR. [75]

In general, the colour flow area of the regurgitant jet is not recommended to quantify the severity of MR, and should be used only for detecting MR. [3, 74, 76]

Figure 5 The effect of Pressure Difference on Regurgitation Severity (adapted from Zoghbi et al., 2017, with permission)

The images from two patients with ischemic MR and eccentric jets directed laterally. Upper panels represent patient with low blood pressure and low MR jet velocity (4,1m/s) reflecting high LA pressure. The bottom panels represent patient with arterial hypertension and high MR jet velocity. MR jet looks almost identical in both patients even though there is a significant difference in MR severity with EROA= 0,3 vs 0,08cm2!!!

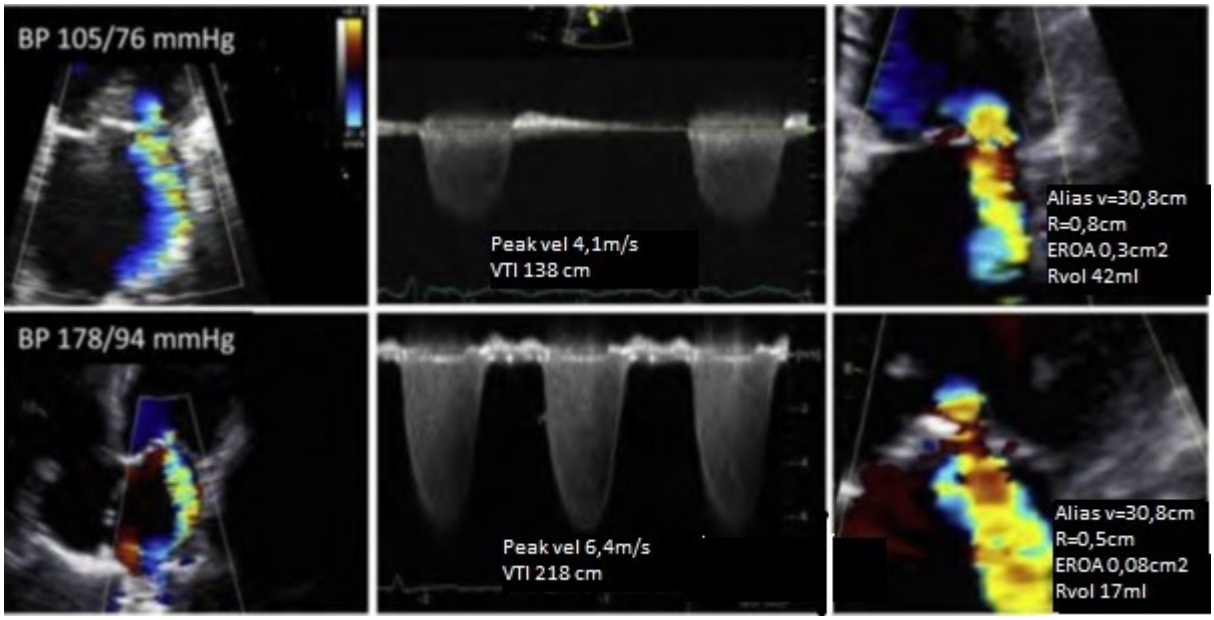

2.1.2. Vena Contracta width (VC width)

The VC is the area of the jet as it leaves the regurgitant orifice; it reflects the regurgitant orifice area. [77]The VC is typically imaged in a view perpendicular to the commissural line as depicted in Figure 6B.

Averaging measurements over at least two to three beats and using two orthogonal planes, whenever possible is recommended. A VC ≤3 mm indicates mild MR; whereas a width ≥7 mm defines severe MR. The concept of VC is based on the assumption that the regurgitant orifice is almost circular. The orifice is roughly circular in primary MR; while in secondary MR, it appears to be rather elongated along the mitral coaptation line and non-circular. [78] Thus, the VC could appear at the same time narrow in the four-chamber view and broad in the two-chamber view. Moreover, conventional 2D colour Doppler imaging does not provide an appropriate orientation of 2D scan planes to obtain an accurate cross-sectional view of the VC. In case of multiple MR jets, the respective widths of the multiple VC are not aditive. Such characteristics may be better appreciated and measured by 3D echocardiography. In secondary MR, an average of VC widths (four- and two-chamber views) has been shown to be better correlated with the 3D VC area. An average value ≥8 mm on 2D echo has been reported to define severe MR for all aetiologies of MR including functional MR. [79]These data need, however, to be confirmed in further studies.

Figure 6 – Measurement of MR PISA Radius and VC width (adapted from Biner et. al., 2010, with permission) A) 4-chamber view to measure PISA radius. Nyquist limit is adjusted to provide optimal visualisation of the mitral regurgitation proximal flow convergence. The PISA radius is measured between the aliasing line of the isovelocity surface and the level of the of the mitral regurgitant orifice. B) Parasternal long axis (PLAX) view to measure vena contracta width. To obtain an optimal view, an observer has to angulate the view to identify three components of the regurgitant flow: the area of proximal flow acceleration, the VC, and the downstream expansion of the regurgitant jet. The VC width is the dimension of the neck between proximal flow convergence and flow expansion in receiving chamber.

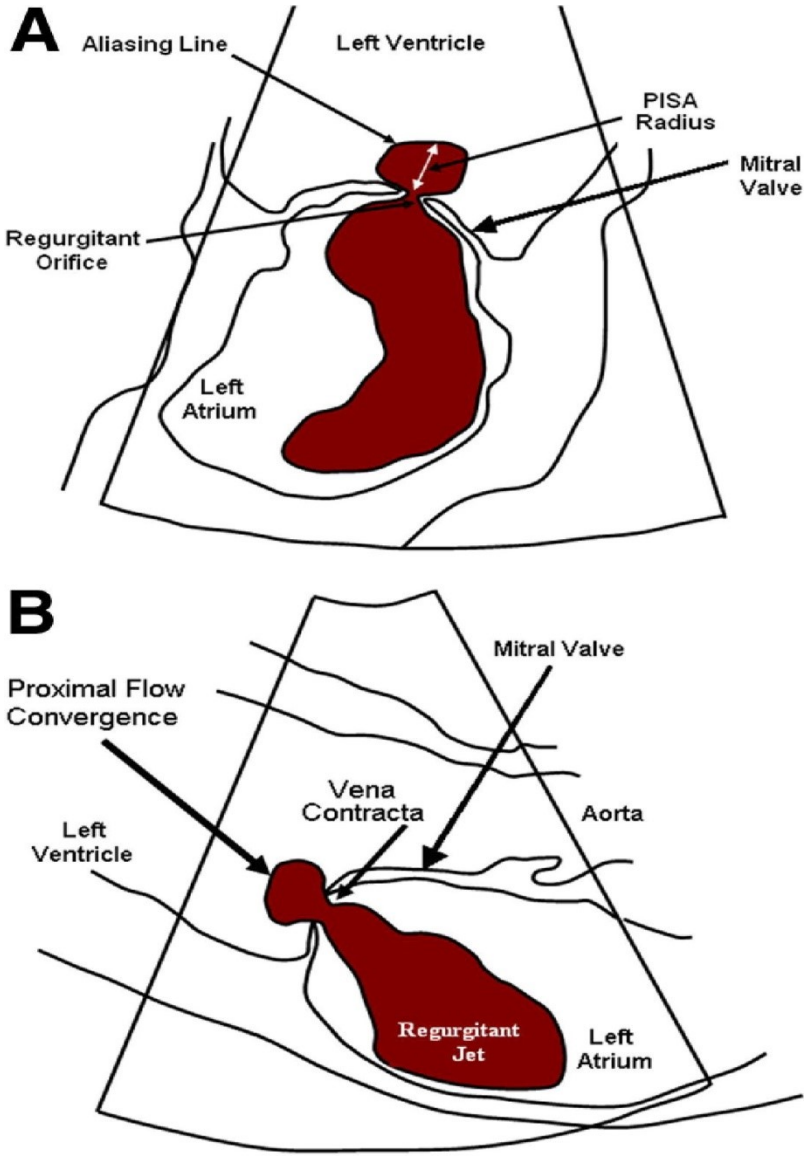

2.1.3. The flow convergence method

The flow convergence method. The flow convergence method is the most recommended quantitative approach whenever feasible. [80] The apical four-chamber view is classically recommended for optimal visualization of the PISA. However, the parasternal long or short-axis view is often useful for visualization of the PISA in case of anterior mitral valve prolapse. The area of interest is optimized by lowering imaging depth and reducing the Nyquist limit to 15– 40 cm/s. The radius of the PISA is measured at mid-systole using the first aliasing. Regurgitant volume and EROA are obtained using the standard formulas.

Qualitatively, the presence of flow convergence at a Nyquist limit of 50–60 cm/s should alert to the presence of severe MR. Grading of the severity of primary MR classifies regurgitation as mild, moderate, or severe, and subclassifies the moderate regurgitation group into 'mild-to-moderate' (EROA of 20–29 mm or an Regurgitant volume (Rvol)of 30–44 mL) and 'moderate-to-severe' (EROA of 30– 39 mm2 or an Rvol of 45–59 mL). Quantitatively, primary MR is considered severe if EROA is ≥40 mm2 and Rvol ≥60 mL. In secondary MR, the thresholds of severity, which are of prognostic value, are 20 mm2 and 30 mL, respectively.[6] EROA is the most robust parameter as it represents a marker of lesion severity. A large EROA can lead to large regurgitant kinetic energy (large Rvol) but also to potential energy, with low Rvol but high LA pressure. The PISA method faces several advantages and limitations. [3, 80] There is very common and unpredictable variation of the MR flow during systole which could be tracked by the colour M-mode for example. Even though not being a rule the PISA radius is most frequently constant in patients with rheumatic MR, frequently increases progressively with a maximum during the second half of systole in patients with mitral valve prolapse and In the presence of functional MR, there is a dynamic variation of the regurgitant orifice area with early and late systolic peaks and a mid-systolic decrease. These changes reflect the phasic variation in transmitral pressure that acts to close the mitral leaflets more effectively when pressure reaches its peak in mid-systole. [81] Individual examples of PISA radius fluctuation is listed in Figure 7.

Figure 7 Individual examples of dynamic changes of the PISA (adapted from Schwammenthal et al., 2002, with permission)

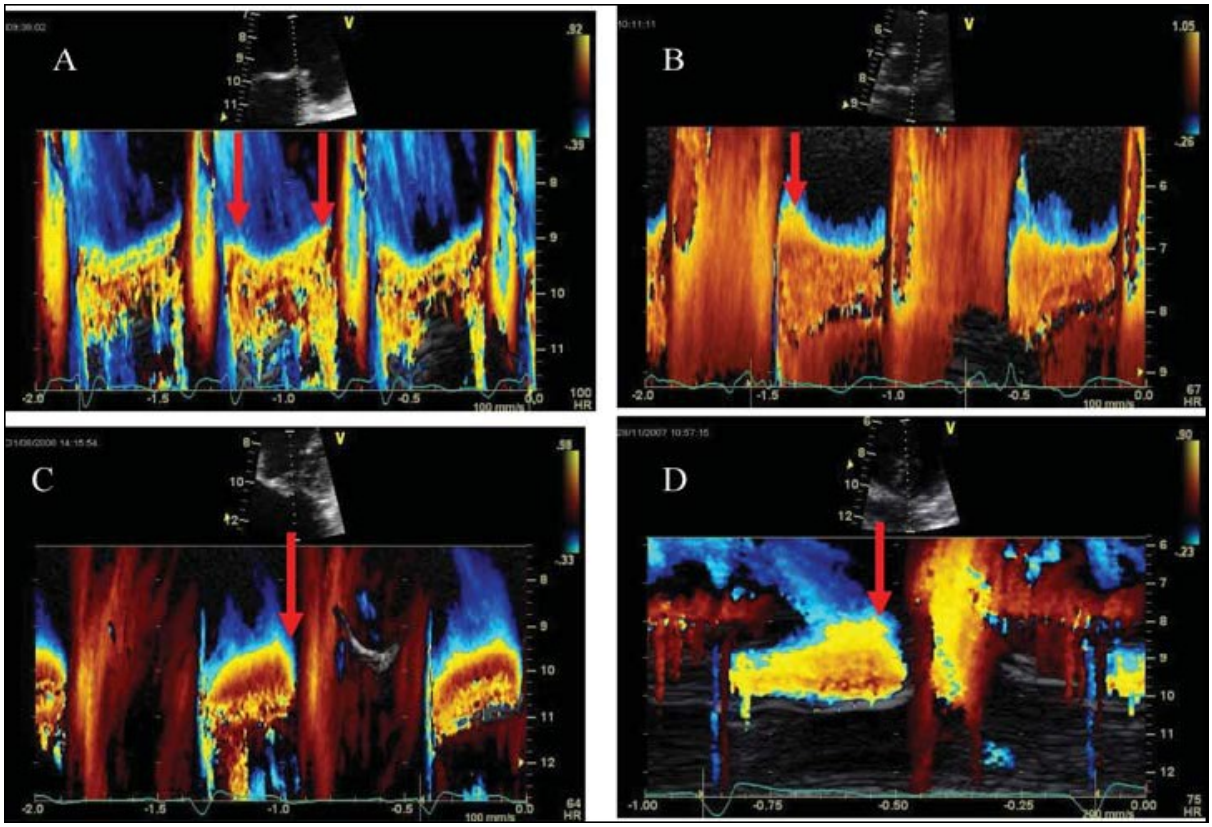

The PISA method is based on the assumption of hemispheric symmetry of the velocity distribution proximal to the circular regurgitant lesion, which may not hold for eccentric jets, multiple jets, or complex or elliptical regurgitant orifices.

Practically, the geometry of the PISA varies, depending on the shape of the orifice and mitral valve leaflets surrounding the orifice. In functional MR, the PISA might look like an ellipsoidal shape and two separate MR jets originating from the medial and lateral sides of the coaptation line can be observed on 2D echo. When the shape of the flow convergence zone is not a hemisphere, the PISA method may underestimate the degree of functional MR, particularly when the ratio of long-axis length to short-axis length of the 3D regurgitant orifice is >1.5. [82] Examples of different shapes of the EROA are illustrated in Figure 8.[74]

Figure 8 Individual examples of typical shapes of effective regurgitant orifices, whereas in functional MR we observe typically oval, elliptic or semilunar shape, in contrast to rather circular shape in primary mitral regurgitation. (from Zoghbi et al., 2017, with permission)

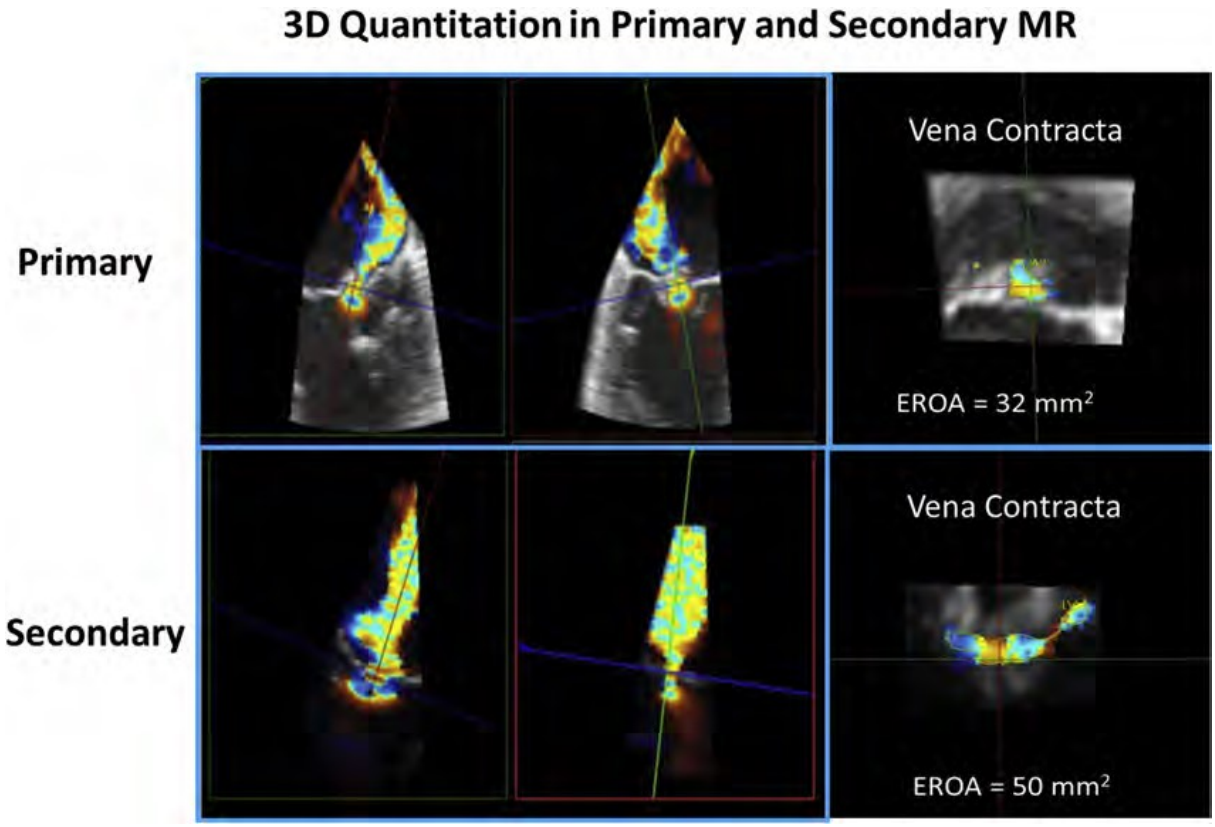

When the EROA is calculated with the hemispheric assumption (using the vertical PISA), the horizontal length of PISA is ignored. In the organic MR, the shape of the PISA is rounder, which minimizes the risk of EROA underestimation. These findings could explain why the threshold used to define a severe functional MR is inferior to that used for organic MR. Careful consideration of the 3D geometry of PISA may be of interest in evaluating the severity of functional MR. [3]

Biner et al., 2010 [83] brought interesting study proving that even highly recommended methods such as PISA method are only modestly reliable with a suboptimal inter-observer agreement for the distinction of the of severe vs. Non-severe MR with reasonable reproducibility only in patients with MR with central jets!

2.1.4. Pulsed Doppler volumetric method

The quantitative PW Doppler method can be used as an additive or alternative method, especially when the PISA and the VC are not accurate or not applicable. This approach is time-consuming and is associated with several drawbacks, with mitral regurgitant volume being obtained by calculating the difference between the total stroke volume and systemic stroke volume (SV).

$SV = CSA \times VTI = \pi d^2/4 \times VTI = 0.785 d^2 \times VTI$; [CSA – cross-sectional area, d- left ventricle outflow tract (LVOT) diameter, VTI- velocity time integral of the flow in LVOT].

Regurgitant Volume = SV regurgitant valve – SV competent valve (or LVOT)

This calculation is inaccurate in the presence of significant aortic regurgitation. In general: The Doppler volumetric method is a time-consuming approach that is not recommended as a first-line method to quantify MR severity.

2.1.5. Anterograde velocity of mitral inflow

Mitral to aortic VTI ratio. In the absence of mitral stenosis, the increase in the transmitral flow that occurs with increasing MR severity can be detected as higher flow velocities during early diastolic filling (increased E velocity). In the absence of mitral stenosis, a peak E velocity of 1.5 m/s suggests severe MR. Conversely, a dominant A-wave (atrial contraction) basically excludes severe MR. These patterns are more applicable in patients older than 50 years or in conditions of impaired myocardial relaxation. The pulsed Doppler mitral to aortic TVI ratio is also used as an easily measured index for the quantification of isolated pure organic MR. Mitral inflow Doppler tracings are obtained at the mitral leaflet tips and aortic flow at the annulus level in the apical four-chamber view. A TVI ratio 1.4 strongly suggests severe MR, whereas a TVI ratio 1 is in favour of mild MR.

2.1.6. Pulmonary venous flow

The pulsed Doppler evaluation of the pulmonary venous flow pattern is another aid for grading the severity of MR). In normal individuals, a positive systolic wave (S) followed by a smaller diastolic wave (D) is classically seen in the absence of diastolic dysfunction. With

increasing the severity of MR, there is a decrease in the S-wave velocity. In severe MR, the S-wave becomes frankly reversed. As unilateral pulmonary flow reversal can occur at the site of eccentric MR jets if the jet is directed into the sampled vein, sampling through all pulmonary veins is recommended, especially during transoesophageal echocardiography. Although the evaluation of the right upper pulmonary flow can often be obtained using TTE, evaluation is best performed using TOE with the pulsed Doppler sample placed 1 cm deep into the pulmonary vein. Atrial fibrillation and elevated LA pressure from any cause can blunt forward systolic pulmonary vein flow. Therefore, blunting of pulmonary venous flow lacks of specificity for the diagnosis of severe MR, whereas systolic pulmonary flow reversal is specific for severe MR.

2.1.7. Continuous wave Doppler of MR jet

Peak MR jet velocities by CW Doppler typically range between 4 and 6 m/s. This reflects the high systolic pressure gradient between the LV and LA. The velocity itself does not provide useful information about the severity of MR. Conversely, the signal intensity (jet density) of the CW envelope of the MR jet can be a qualitative guide to MR severity. A dense MR signal with a full envelope indicates more severe MR than a faint signal. The CW Doppler envelope may be truncated (notched) with a triangular contour and an early peak velocity (blunt). This indicates elevated LA pressure or a prominent regurgitant pressure wave in the LA due to severe MR. In eccentric MR, it may be difficult to record the full-CW envelope of the jet because of its eccentricity, whereas the signal intensity shows dense features.

2.1.8. Integrating indices of severity

The echocardiographic assessment of MR includes integration of data from 2D/3D imaging of the valve and ventricle as well as Doppler measures of regurgitation severity. Effort should be made to quantify the degree of regurgitation, except in the presence of mild or obviously severe MR. Both the VC width and the PISA method are recommended. Adjunctive parameters help to consolidate about the severity of MR and should be widely used particularly when there is discordance between the quantified degree of MR and the clinical context. For instance, a modest regurgitant volume reflects severe MR when it develops acutely into a small, non-compliant LA and it may cause pulmonary congestion and systemic hypotension.[3]

3. Basic principles of flow quantification in valvular heart disease

The basic principle of the flow quantification is derived from the measurement of flow velocity and the cross-sectional area of the flow – when both multiplied providing flow rate. When the flow rate is integrated through the time we get flow volume.

$RV \approx EROA \int_{TriTr} VCW dt = EROA \cdot TVI$

TVI – total velocity integral (Continuous Wave Doppler transducer beam Vcw over time interval during the regurgitation phase), EROA – effective regurgitant orifice area

Where

$EROA = 2\pi r^2 Va / VMR$

r – radius of the isovelocity surface corresponding to the Nyquist aliasing velocity Va, VMR is peak mitral regurgitation through the orifice.

This formula is based on the principle of the conservation of the mass and assumption, that the isovelocity surfaces in the flow convergence zone form hemispheres. [84, 85]

Several studies have shown that that single radius hemispherical formula under-estimates the true MR severity due to the fact that the regurgitant orifice is often non-circular, slit-like or arcuate and therefore the assumption of hemispherical shape of the flow convergence is not right. [86-88]

However, apart from laboratory conditions, all the measurements become very challenging in the situation when a blood volume moves from one heart chamber to another by passing through the diseased valve limiting the whole concept as described above.

Three important features were defined by Buck et al.[89] For the blood crossing the diseased valve:

1) an asymmetric cross-sectional area of the flow

2) an irregular-shaped field of flow or flow jet distal to the heart valve

3) complex dynamic pattern of the flow during a cardiac cycle.

Recently developed 3D colour Doppler imaging methods may help to overcome the limitations of 2D colour Doppler methods.

4. Three-dimensional echocardiography

4.1. Introduction

Three-dimensional (3D) echocardiographic (3DE) imaging is a major innovation in cardiovascular ultrasound. Advancements in computer and transducer technologies allow real-time 3DE acquisition and presentation of cardiac structures and blood flow from any spatial point of view. The usefulness of 3DE was proven in 5 categories: 1) the evaluation of cardiac chamber volumes and mass, avoiding geometric assumptions; 2) the assessment of regional left ventricular wall motion and quantification of systolic dyssynchrony; 3) presentation of realistic view of heart valves; 4) volumetric evaluation of regurgitant lesions and shunts with 3DE colour Doppler imaging; and 3DE stress imaging.

However, it would be a long way for full implementation of the 3DE methods to the routine clinical practice. A full understanding of its technical principles and systematic approach to image analysis and acquisition are required. [90]

4.2. Instrumentation

The milestone in the history of real-time 3DE was reached in the year 2000 when fully sampled matrix-array transducers were introduced, providing reasonable real-time imaging of the beating heart in free dimensions. 3DE matrix-array transducers are composed of thousands of piezoelectric elements operating in frequencies from 2-4MHz or 5-7MHz for transthoracic echocardiography resp. Transoesophageal echocardiography.

4.3. Data Acquisition

Basically, there are two methods for 3DE data acquisition: real-time or live 3DE imaging and electrocardiographically triggered multiple-beat 3DE imaging.

Real-time 3DE allows acquisition of multiple pyramidal datasets per second in a single heartbeat. Live 3Din usually available in several modes: live 3D narrow volume, live 3D zoomed, live 3D wide angled (full volume) and live 3D colour Doppler. In general, this

method overcomes the limitations imposed by rhythm disturbances or respiratory motion but at cost of poor temporal and spatial resolution.

In contrast, multiple-beat echocardiography provides images of higher temporal resolution. Narrow volumes of data over several heartbeats are acquired and subsequently, they are all put together to create a single volumetric data set. However, when data acquisition is gated to the surface ECG, it is prone to the stitching artefacts from the patient, breathing or irregular cardiac arrhythmias. [90]

Figure 9 With stable cardiac position throughout subvolume acquisition during electrocardiographically triggered multiple-beat 3DE acquisition, no stitch or gating artifacts are visible when the subvolumes are joined. This can be seen on either the 2D cut plane perpendicular to the sweep plane (top left) or the 3DE volume (bottom left). Unstable cardiac position during subvolume acquisition caused by patient respiratory motion or irregular cardiac rhythm results in stitch artifact, where the individual subvolume components constituting the 3DE image can be seen on the 2D cut plane (top right) and the 3DE volume (bottom right). AV, Aortic valve; MV, mitral valve.(adapted from Lang et al., 2012, with permission) [90]

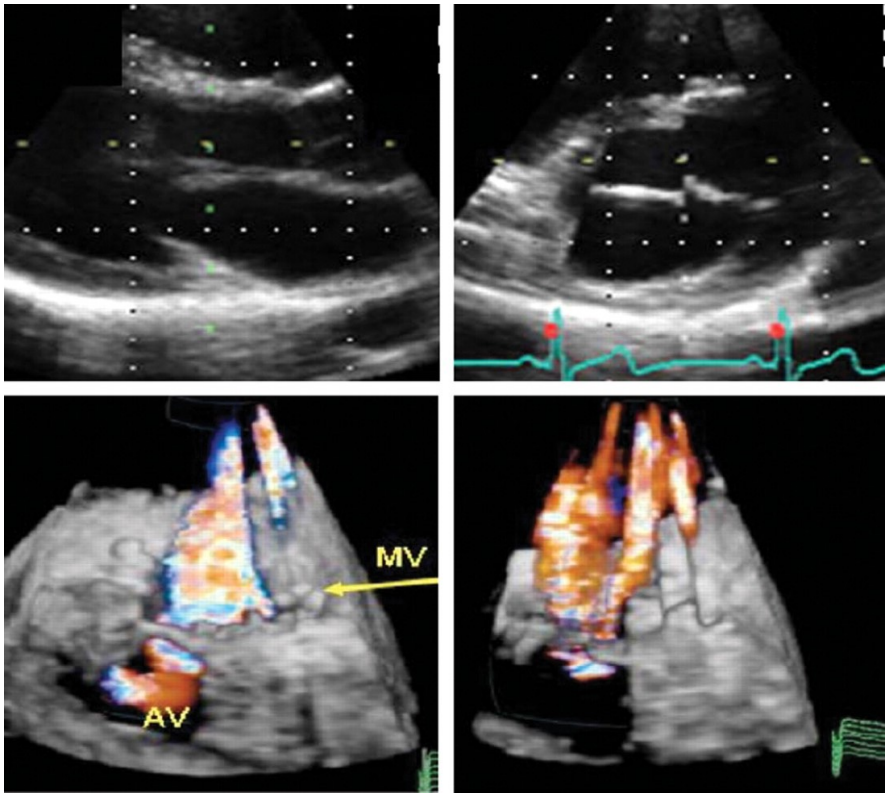

4.3.1. Data Acquisition Modes

1) Real-Time 3D mode with narrow sector: allows real-time display of pyramidal volume. It is usually insufficient to visualise the whole structure we want to see, but its high spatial and temporal resolution allows accurate diagnosis when step by step visualisation is possible.
2) Focused Wide Sector – ZOOM: permits a focused, wide sector view of cardiac structures, but when enlarged, a significant drop in spatial and temporal resolution is observed.
3) Full Volume Gated acquisition: enables to assess the largest acquisition sector possible, which is ideal for global imaging of structures such as left ventricle, mitral valve or aortic root for example with very good spatial and temporal resolution (above 30Hz) for the detailed analysis. Usually, we get large data set which has to be further cropped and trans-sected in multiple planes to "remove" unnecessary tissue or structures to visualise what we aim for with special off-line analysis software.
4) Full Volume with Colour Flow Doppler: at first, when introduced, 3DE colour Doppler imaging could be acquired using a full volume gated reconstruction technique. 7-14 pyramidal volume slabs were gated to ECG to make a 3D composite volume at a frame rate of 15-25Hz. When the last guidelines for the 3D echocardiography were introduced [90] – new vendors allowed us the acquisition of as low as 2 beats, and further our study could be done because of possible real-time 3D colour Doppler analysis – of course – at costs of temporal resolution.

The battle for the spatial and especially temporal resolution improvement is in hands of vendor companies because any acquisition mode in the necessity of gating is very prone to artefacts and in patients with irregular heart rhythm, such as atrial fibrillation, almost impossible to use.

4.3.2. How to avoid artefacts related to gated datasets

As mentioned, respiratory movements and rhythm disturbances are very challenging. There are a few rules to follow:

1) To improve spatial resolution, the pyramidal volume dataset must be as small as possible to encompass all the structures we want to see and not more.

2) For the temporal resolution, it is not reasonable to increase the frame rate just because you can, at the cost of multiple beat gating and a higher chance for the stitching artefacts. One should also pick ECG signal of high and stable quality to avoid false ECG signal tracking by the vendor.
3) Breathing artefacts: if possible, the patient should hold breath for the time of acquisition. It is very useful to check the image quality during respiration to find the best image quality during a respiratory cycle. In some patients, it may be with complete exhalation, however, interestingly, in some in almost peak inhalation.
4) The golden rule applies in general: Before 3D image acquisition, check the image quality of the 2D datasets, because suboptimal 2D images always result in even more suboptimal 3D datasets. [91]

4.3.3. 3D optimisation

As with 2D echocardiography, optimising lateral and axial resolution remains equally important during 3DE acquisition. In general, low gain setting will result in echo dropouts, which cannot be restored during post-processing. Usually, the gain and compression settings should be set in mid-range (50 units) and optimised with slightly higher time gain controls (time gain compensation) to enable the greatest flexibility for post-processing gain and compression. We prefer a slight overcompensation of the brightness of the image to using of the power-output gain adjustment.

4.3.4. 3DE Image Display

1) Cropping

   The concept of cropping is the “holy grail“ of 3D echocardiography. 3D echocardiography requires good orientation in anatomy and that the structure we follow has to be “cut out“ of the dataset, like the sculpture from the solid rock. If you want to see, for example, mitral valve from full volume dataset, you have to crop the base and the apex of the heart (its left side) to enjoy looking into the mitral valve from the atrial or ventricular side. Echocardiographer has to change the cross-sectional approach to that of anatomist or surgeon, who also looks into intra-cardiac structures after exposing them. 3D cropping can be done during post-processing or during data acquisition. It seems reasonable to crop the dataset during the

examination because by doing that, we increase temporal and spatial resolution. On the other hand, the pre-cropped dataset may have drawbacks in terms of missing parts of the datasets revealed during post-processing.

2) Post-Acquisition Display

3D dataset can be viewed interactively with several 3D visualisations and software packages. The choice of the display technique is related to the clinical application.

a) Volume rendering

This technique preserves all 3D information and projects it, after processing onto 2D plane for viewing. All voxels along each light beam are weighted to obtain voxel gradient intensity that is integrated with different levels of opacification, shading and lighting – allowing an individual structure to appear solid or transparent. Several shading techniques (grey level gradient coding, texture coding) are used to generate a 3D display of the depths and textures of cardiac structures. [92] Volume rendering provides complex spatial relationships in a 3D display which is useful for evaluation of the valves and adjacent anatomical structures.

b) Surface rendering

A surface rendering shows the surface of structures or organs in a solid appearance. To use this technique, segmentation of the data-set can be applied to identify the structure of interest. Surface rendering of selected structures is obtained by manual tracing or by semi-automatic border detection algorithms to trace the endocardium in cross-sectional images generated from the 3D dataset. These contours are combined together to make 3D shape that can be visualised as a solid or a wireframe object to create a 3D perspective. This technique is typically used for the stereoscopic presentation of the left ventricle for the visual assessment of ventricular shape, volume and function – including volume changes during a cardiac cycle. However, surface rendering frequently fails to provide details of cardiac structures or texture. [93]

c) Tomographic slices

2D echocardiography is typically based on tomographic slices of the heart and the virtual cut plane depends completely on the operator experience and the acoustic window. On contrary, the volumetric dataset obtained by 3D

echocardiography can be sliced or cropped to obtain virtually any 2D acoustic window, completely avoiding possible drawbacks and limitation of 2D echocardiography in terms of cutting planes. It is quite common that for example in left ventricle diameters throughout cardiac cycle, two operators refer quite a different diameter and especially wall thickness due to oblique cut of the tubular structure of the left ventricle. With 3D dataset, we may precisely measure left ventricle diameters in longitudinal or transverse planes in true long or short axis views – significantly improving inter-individual variability and validity of the measurements. Several slicing methods are available. In arbitrary plane cut operator may orient the cutting plane in any direction in a way of interest. The simultaneous orthogonal 2D slices mode consists of two or three planes displayed simultaneously (coronal, sagittal, transverse) or even multiple parallel equally spaced slices. This technique was validated also in structural heart diseases in patients with atrial or ventricular septal defects, mitral valve stenosis or mitral valve regurgitation for the 3D colour Doppler flow analysis enabling reproducible a valid assessment of the pathologies. [78, 94, 95] Ventricular function analysis during stress echocardiography was also described enabling to follow reproducibly the same ventricular segment during cardiac cycle. [96]

4.4. Three-dimensional (3D) Colour Doppler Acquisition

4.4.1. Data acquisition in TTE and TEE

Similar to conventional 2D echocardiography, colour Doppler imaging is superimposed into 3D echocardiography morphological dataset. Three-dimensional colour Doppler acquisition is performed with live 3D or multiple-beat full-volume acquisition, which provides larger data volumes but it is limited by stitching artefacts. In contrast live 3D colour Doppler acquisition is not limited by stitching artefacts at the costs of smaller colour Doppler volumes and lower frame rates. 3D colour Doppler data acquisition is feasible with transthoracic (TTE) and transesophageal (TEE) echocardiography examination. TEE provides better colour Doppler flow analysis and is recommended for more detailed colour flow analysis. But TEE is of no use for the stress echocardiography testing especially for the purposes of our study with dynamic stress on ergometer. Similar to what occurs during non-colour Doppler

3D dataset acquisition, the size and location of the 3D colour Doppler volumes should be carefully defined according to the flow region to be analysed. The example of colour Doppler 3D datasets throughout the systole is depicted on Figure 10.

Figure 11 Individual dynamic changes of mitral valve regurgitation throughout the systole in real time three-dimensional colour Doppler imaging. (Dr.Vecera)

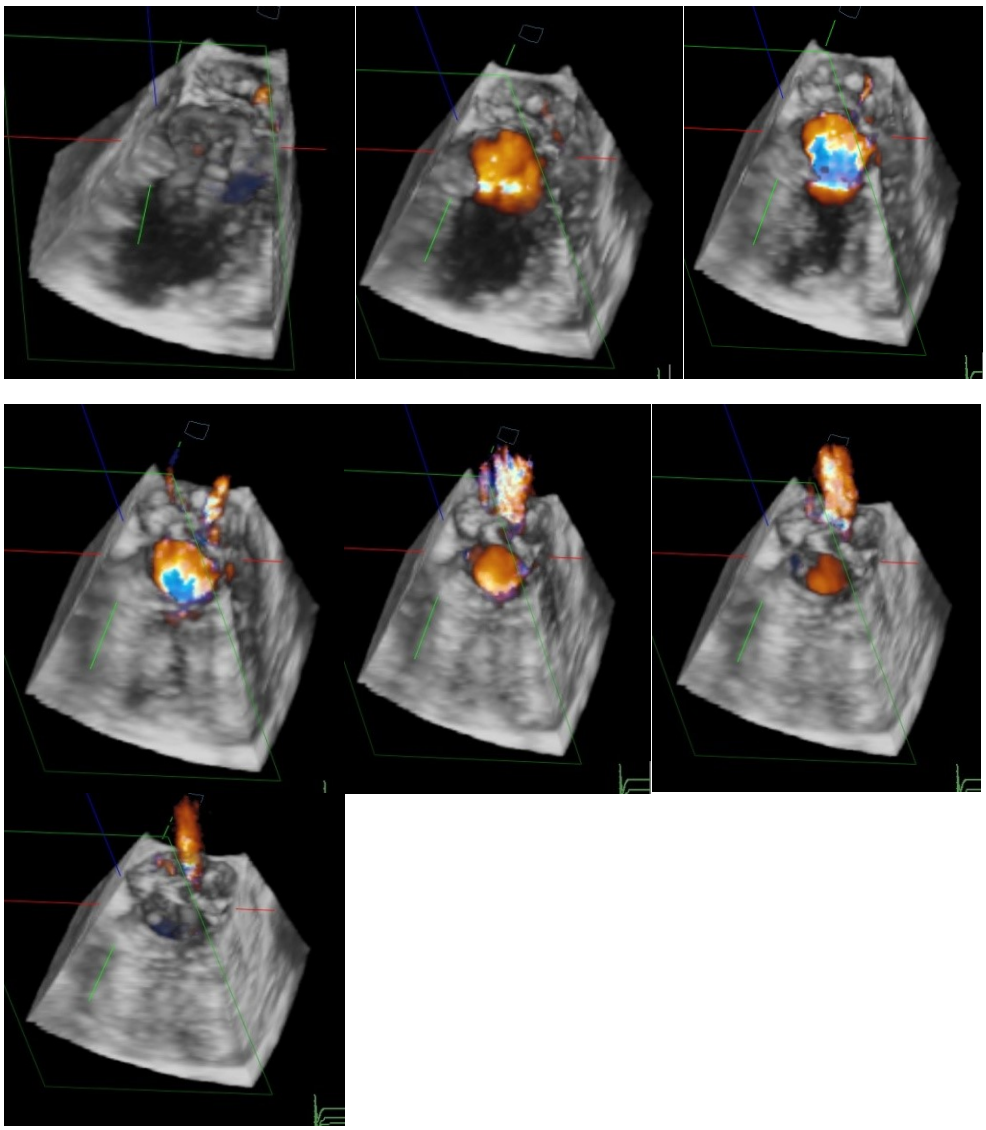

4.4.2. Cropping methods

Cropping flow analysis includes distal jets, the proximal flow field of valvular flow regurgitation, and flow through heart defects such as ventricular or atrial septal defect. Cropping of 3D colour Doppler datasets follows the same principles as non-colour Doppler data set cropping and is determined mainly by the analysis intended. For the regurgitant jets, it is recommended to crop the 3D colour Doppler data set to show two long axis views of the jet: one with the narrowest and one with the broadest width of the jet. This display should – and for the sake of our study – must include a short-axis view of the jet at the level of the vena contracta. Alternatively, colour Doppler flow can be displayed using multiple slice representation extracted from the 3D colour Doppler data set. The example of VCA analysis is depicted on Figure 11.

Figure 11 Individual example of colour Doppler three-dimensional dataset in the patient with mitral valve regurgitation. We may see on the left side two sub-images showing individually both cropping planes located perpendicularly to the flow in two orthogonal planes in the narrowest part of the vena contracta – which then becomes apparent as depicted on the right side of the lower panel. (Dr.Večeřa)

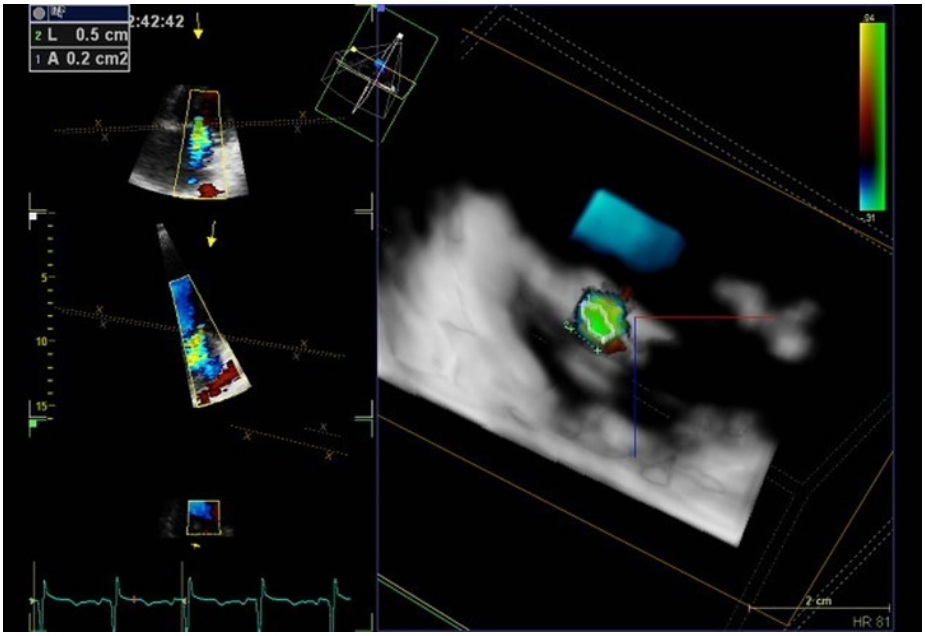

1) Orientation and Display

Understanding the orientation of colour Doppler flow within the displayed views is clinically important. It is recommended displaying the 3D colour Doppler dataset in at least two different views with known orientation to each other as indicated by different coloured cutting planes to help with the orientation. It is also reasonable and recommended to display 3D colour Doppler data together with characteristic anatomic 3D information using standard views.

2) Limitations

The basic limitation of the 3DE colour Doppler acquisition includes relatively poor spatial and temporal resolution, however novel hardware and software advancements are promising. Currently, live 3D colour Doppler is limited to small colour Doppler volumes usually with the limited temporal resolution to 10-15 voxel/sec. If we focus on a relatively limited volume such as proximal isovelocity flow or vena contracta area it is large enough – such as for the purpose of our study. Alternatively, multiple-beam full-volume acquisition of colour Doppler provides larger colour Doppler volumes and volume rates (up to 40 voxel/sec) but it is limited by stitching artefacts, resulting in significant displacements between different subvolumes. [90]

4.5. 3D stress echocardiography

Three-dimensional stress echocardiography represents a major advancement for the clinical evaluation of ischemic heart disease. The most common stress modalities (exercise, dobutamine, dypyridamol) were tested with reasonable sensitivity, specificity and high feasibility for the detection of coronary artery disease native or with contrast imaging. Colour Doppler 3D imaging during stress was not studied and published previously.

4.6. Current status of 3D echocardiography

According to the latest version of EAE/ASE Recommendations for Image Acquisition and Display Using Three-Dimensional Echocardiography (Lang et al., 2012) there is only limited number of 3D examination recommended for the clinical practice with several areas of interest in different levels of knowledge and evidence:

1) Recommended for Clinical Practise: Left ventricle assessment of the volume, ejection fraction, Mitral valve anatomy, mitral valve stenosis and guidance of transcatheter procedures
2) Promising clinical tool: Left ventricle mass, right ventricle volume and ejection fraction, aortic valve stenosis and anatomy
3) Areas of active research: left ventricle shape, dyssynchrony, left atrial volume, mitral valve regurgitation, and prosthetic valves. [90]

5. The three-dimensional colour Doppler imaging concept

5.1. Vena Contracta Area (VCA) concept

5.1.1. Introduction

The holy grail of the concept is located at the narrowest portion of the regurgitant jet, just distal to the regurgitant orifice. This segment of the regurgitant jet corresponds hemodynamically to the effective regurgitant orifice area (EROA). In the clinical settings the VCA can be up to 40% smaller than the anatomical orifice and the factors that influence the magnitude of this on-going flow contraction and its area respectively, including the geometry of the anatomical orifice (which highly variable) and the fluid viscosity (less variable).[97] The location and the size of the VCA are highly dependent on the geometry of the mitral valve orifice and largely independent of flow rate. [77] As mentioned previously current guidelines suggest that regurgitation severity can be approximated by measurement of the diameter of the VC. [3] However, when the regurgitation occurs through the asymmetric orifice, such as in functional MR, the validity of the 2D diameter of such complex geometry is limited. [98-100]

With the recent development of the 3D colour Doppler imaging we can now provide any plane cropping of the volumetric data to identify the true cross-sectional area of the Vena Contracta – therefore a direct measure of the EROA! [90]

5.1.2. Setting up the concept for the clinical application

Several studies have built the case for the routine use of VCA to estimate a single EROA in patients with either organic or secondary-functional MR. In the early study by Little et al, 3D transthoracic echo was used to demonstrate that 3D VCA measurement was feasible and quick to perform and demonstrated a better relation to Doppler-derived EROA than did 2D VC diameter in patients with clinically significant MR. [101] Khanna et al. Initially demonstrated colour Doppler real time 3DE as a feasible to provide direct visualisation and planimetry of the VCA of the regurgitant jet. [98]Kahlert et al., first provided evidence, that RT3DE overcomes the limitations of 2D measurements of 2D VC width by direct assessment of the size and shape of the VCA and demonstrated differences in VCA asymmetry among different aetiologies of MR. [100]

Figure 12 shows three examples of different shapes of VCA in patients with secondary functional MR reflecting an unpredictable shape of the effective regurgitant orifice, hence challenging the assumption, that EROA has a round shape (Dr.Večeřa)

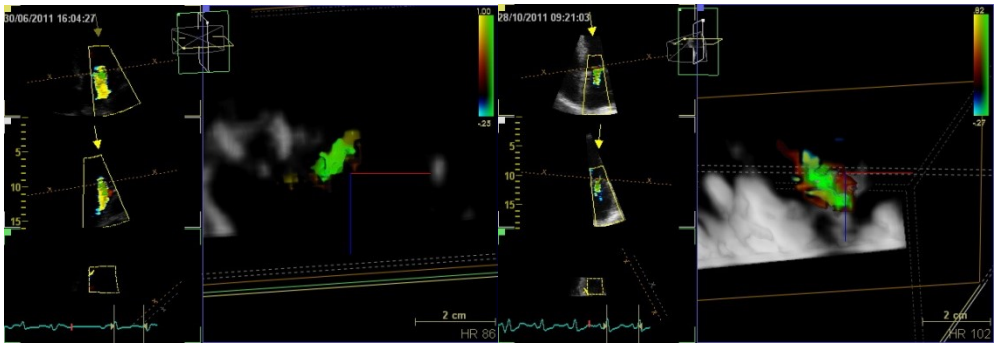

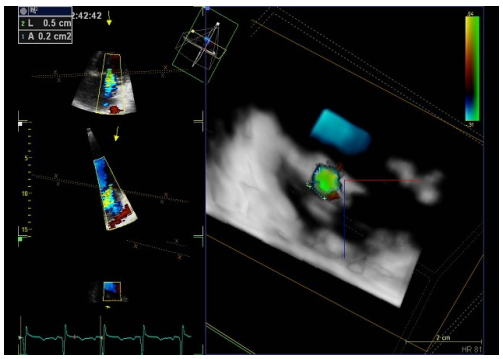

In the majority of the patients, we observe elongated, semilunar-shaped VCA – as depicted in Figure 12.

Several studies recently compared 3D VCA measurements with other methods particularly for the quantification of the MR demonstrating an increasing superior accuracy of 3D measurements over 2D ones the more asymmetric the VCA was. Summarised in table 3.

Marsan et al. Compared VCA derived regurgitant volume with cardiac magnetic resonance (CMR) measures of regurgitant volume and showed volume difference between techniques of <1ml/beat. [102] Shanks et al. Also compared VCA (from TEE) with CMR derived Rvol and showed that 2D TEE significantly underestimated the EROA and regurgitant volume by 22% compared to CMR or 3D TEE. [103]Finally, Zeng et al. Compared direct planimetry of the VCA with an integration of 2D methods as a reference. A VCA cut off of 0.41cm² reliably differentiated severe from moderate MR. This VCA cut off is consistent with cut off value of 0.4 cm² in current guidelines for the severe primary MR. [60, 76]

In multi-jet mitral regurgitation, recently Hyodo et al. Tested quantification of multiple jets using VCA measurements from 3DE in patients with functional MR and at least two distinct jets compared with unique measurements of Rvol derived from 3DE left ventricle stroke volumes subtracted by thermodilution method derived systemic stroke volume with impressive reference correlationn of r=0.91 whereas 2D VC only r=0.46.

Figure 13 Individual examples of multi-jet FMR with apparent two and three jet vena contractas by 3D colour Doppler echocardiography. On the right side of both images we may observe two, respectively three VCA of the regurgitant jets – whereas on the left side you may observe 2D acquisition of regurgitant jets, where only a single jet is apparent !! (Dr.Večeřa)

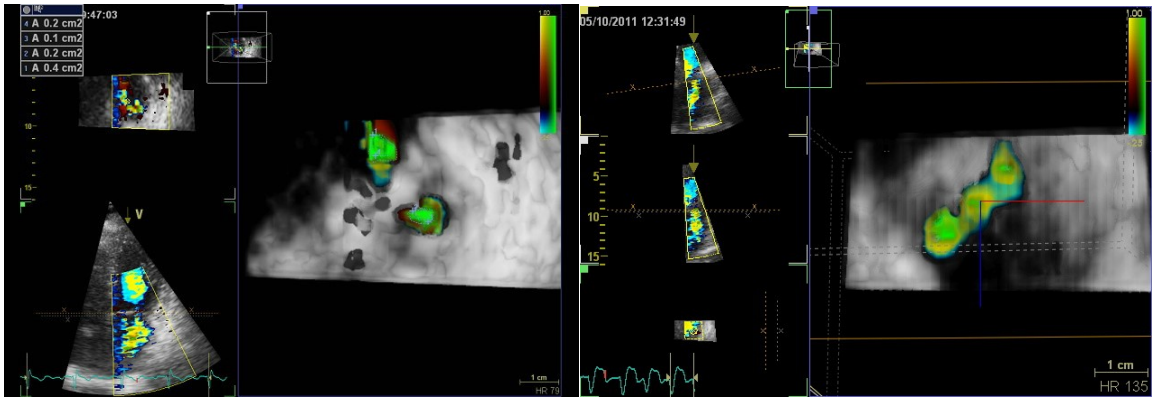

Therefore, we may conclude, that VCA can be accurately assessed by 3D TTE or 3D TEE methods and that this directly measured area correlates well with accepted 2D Doppler and CMR standards used to quantify MR severity. [97] And we also believe that this analysis is possible also in patients during exercise echocardiography. As presented in Figure 14, revealing the very first examples of dynamic changes of 3D derived vena contracta area during exercise in patients with secondary mitral regurgitation.

Figure 14 Individual examples of exercise-induced increase of VCA (1A, 1B) versus stable small VCA (1C, 1D). VCA (white ellipse) was assessed using manual planimetry at the closest frame to mid-systole. Care was taken to circle the central area of the high-velocity flow while avoiding the low-velocity colour flow signals at the periphery. VCL was measured as the maximal VCA diameter. In this patient (1A), a relatively large ellipsoid VCA was observed at rest (1A) despite the small colour-coded regurgitant jet area (right panel) and "mild" appearance of FMR. Figure 1B shows significant increase in VCA corresponding to significant FMR during low-load exercise (50 W). Figure 1C and 1D show an example of a patient with the small circular VCA both at rest and during exercise, respectively, reflecting stable mild-to-moderate FMR. On the right side of each 3D image is 2D colour Doppler image revealing concomitant 2D colour Doppler PISA and regurgitant jet. (Dr.Večeřa, with permission)

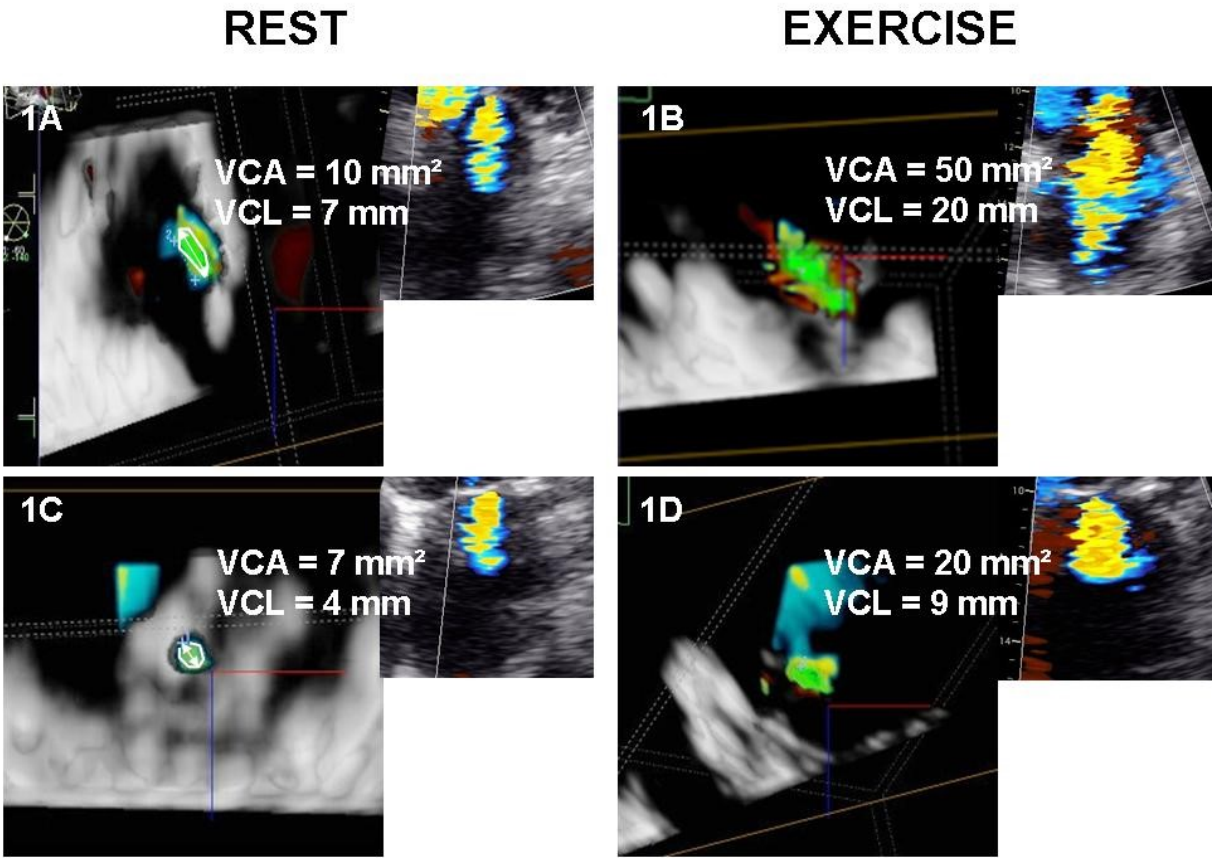

Table 3 Overview of the studies validating 3D vena contracta area measurement against 2D methods and independent methods (adapted from. Buck et. Al., 2015, with permission [89])

Study	No. Of patients	Scan method	Aetiology	Comparison method	Correlation/agreement (mean diff.±SD)	Inter-/intraobserver variability
Khanna et al. (2004)[98]	44	TTE	Not reported	Ventriculographic grading	r=0.88; limits of agreement not reported	r^2=0.99/ r^2=0.97
Iwakura et al. (2006) [82]	109	TTE	FMR 63%	EROA by 2D PISA and by 2D QD	r=0.93 with 2D PISA; 0.07±0.1cm² r=0.91 with 2D QD; 0.05±0.1cm²	8,6%/9.0%
Kahlert et al. (2008) [100]	57	TTE	FMR 36%	EROA by 2D and 3D PISA	r=0.96 with HE PISA; -0.09±0.14cm² r=0.93 with HS PISA; -0.2±0.2cm²	0.04 cm²/..
Little et al. (2008) [101]	61	TTE	FMR 44%	EROA by 2D QD	r=0.85; limits of aggr. NR	0.03/0.05 cm²
Yosefy et al. (2009)[79]	49	TTE	FMR 58%	EROA by 2D QD	r^2=0.86; 0.04±0.06 cm²	0.03/0.02 cm²
Marsan et al. (2009)[102]	64	TTE	FMR 100%	Rvol by CMR	r=0.94 (bias: -0.08ml; 7.6ml/-7.7ml)	0.06/0.04 cm²
Shanks et al.(2010)[103]	30	TEE	FMR 53%	Rvol by CMR	NR; 63±41ml (3DE) vs. 65±43ml (CMR)	0.01/0.01 cm²
Zeng et al. (2011)[104]	83	TTE	FMR 47%	Integrated 2D methods	r=0.88; NR	0.03/0.04 cm²
Hyodo et al. (2012)[105]	60	TEE	FMR 100%	EROA from 3D left ventricular volume and thermodilution data	r=0.90;-0.05±0.06 cm²	0.06/0.05 cm²

HS hemispheric; HE hemielliptic; FMR functional mitral regurgitation; QD quantitative Doppler; Rvol regurgitant volume; CMR cardiac magnetic resonance; EROA effective regurgitant orifice area; 2DE two-dimensional echocardiography; 3DE three-dimensional echocardiography; PISA proximal iso-velocity surface area

5.1.3. VCA method limitations and doubts

The size of VC is considered to be independent of flow rate and dependent on the size of the regurgitant orifice. [77, 101, 106] In clinical practise, the accuracy of 3D colour Doppler measures of their VCA can be affected by several user and machine settings, such as colour

Doppler gain and algorithms employed by the image display software, which controls whether a give region of volumetric data at the tissue/blood interference is displayed as either tissue or flowing blood. If the write priority algorithm is adjusted in favour of colour Doppler, then the VCA appear larger. Only some vendors provide user control of these settings. Another important issue bring gain settings adjustments, because these may have a profound impact on the size of the visible VC area, but have no effect on the true VC area. Usually, we keep the tissue gain setting in mid-range of 50% to minimise the variability in VCA measurements – the same setting as reported by the guru of 3D echocardiography dr. Little in his laboratory. [97] We also have to acknowledge that the correlation of the standard MR severity measurements with 3DE is poorest in mild MR, probably due to the limited spatial resolution of the VCA measurements when the flow is the smallest limiting the manual or automatic tracking of the borders of VCA.

5.2. The three-dimensional colour Doppler PISA concept

Compared to VCA, the proximal isovelocity surface area (PISA) is more complex entity. However, the limitations of the 2D colour Doppler application for the PISA measurements pertains the same as for 2D vs. 3D VC measurements. As mentioned previously its hemodynamic assumption of hemispherical shape of isovelocities in the proximal flow field holds only for circular regurgitant lesion. Previous studies demonstrated that the shape of PISA is rather hemi-elliptic leading to systematic underestimation of EROA and the regurgitant flow measured by the hemispheric PISA method leading to the clinically significant underestimation of MR severity in up to 45% patients. [82, 99, 100]

Hemi-elliptic PISA can be obtained from RT3DE datasets using PISA widths, lengths and radius for the PISA surface calculation. Unfortunately, the hemi-elliptic formula behind is complex and is not routinely implemented in current 3D vendors and its software – as it was also in the case of our echocardiographic laboratory. Several research groups validated in vitro and in vivo methods for the 3D PISA shapes and surface measurements, even semiautomatic and significantly improved accuracy of 3D PISA estimates of EROA and regurgitant flow. The overview of the most important studies related to the 3D PISA is in Table 4.

Especially novel and commercially available methods for automated 3D PISA quantification using single-beat RT3DE colour Doppler datasets give us a hope for the future. However, there is still concern that current transthoracic colour Doppler 3D methods image quality might not be sufficient enough for valid application of this automated analysis in an acceptable proportion of patients in routine clinical practice. It would be of extremely useful to find automated 3D PISA analysis enabling to measure MR flow volume by integrating the dynamically changing PISA over systolic time as described by Buck et al. [107]

Table 4 Overview of clinical studies validating 3D PISA measurements against 2D methods and independent methods (adapted from. Buck et. Al., 2015, with permission [89])

Study	**No. Of patients**	**Scan method**	**PISA method**	**Aetiology**	**Comparison method**	**Correlation/agreement (mean diff.±SD)**	**Inter-/intraobserver variability**
Yosefy et al. (2007)[99]	50	TTE	HS/HE	Not reported	EROA by 2D QD	HEPISA: r^2=0.87; HSPISA: r^2=0.59	HE 5.3%; HS 4.1%
Kahlert et al (2008) [100]	57	TTE	HS/HE	FMR 36%	EROA by 3D VCA	HEPISA: r=0.96; -0.09±0.14 cm² HSPISA: r=0.93; -0.20±0.20 cm²	NA
Plicht et al. (2008)[108]	23	TTE/TEE	HS/HE	FMR 47%	Rvol by CMR	HEPISA: r=0.89; -17.4±9.4ml HSPISA: r=0.81; -11.7±7.4ml	NA
Matsumura et al.(2008)[78]	30	TTE	HS/HE	FMR 100%	EROA by 2D QD	HEPISA: r=0.75; bias –0.1 cm² HSPISA: r=0.69; bias -0.18 cm²	HE 0.06/0.04 cm² HS 0.07/0.03 cm²
Grady et al.(2011)[109]	33	TTE	Automated 3D PISA	Not reported	EROA by 3D VCA	r=0.61 (p=0.002)	NA
De Augustin et al. (2012)[110]	33	TTE	Automated 3D PISA	FMR 24%	EROA by 2D QD and by 3D VCA	r=0.96 with 2D QD; -0.05±0.09 cm² r=0.99 with 3D VCA; -0.03±0.04 cm²	ICC 0.96/0.92
Thavendiranthan et al.(2013)[111]	30	TTE	Automated 3D PISA	FMR 30%	Rvol by CMR	Mean peak PISA: r=0.87; - 15.3±12.8ml integrated PISA: r=0.92; - 1.4±9.2ml	2.2/0.7ml
Choi et al. (2014)[112]	211	TTE	Automated 3D PISA	FMR 47%	Rvol by CMR (n=52)	R=0.97; - 0.9±6.9ml	0.8/0.5ml
Schmidt et	93	TTE	Automated	FMR 80%	Metascore	Mean 3D EROA: AUC	NA

al.(2014)[113]			3D PISA		for MR severity	0.91; peak 3D EROA: AUC 0.84; EROA 2D PISA: AUC 0.75	

HS hemispheric; HE hemielliptic; FMR functional mitral regurgitation; QD quantitative Doppler; Rvol regurgitant volume; CMR cardiac magnetic resonance; EROA effective regurgitant orifice area; 2DE two-dimensional echocardiography; 3DE three-dimensional echocardiography; PISA proximal isovelocity surface area; VCA vena contracta area; AUC area under curve, ICC interclass correlation coefficient

5.3. Comparison of 3D VCA and EROA by 3D PISA

There are only limited data for the comparison of both methods with no prognostic data and conflicting results.

6. Original study and data analysis

6.1. Background and Aims of our prospective study

Severe functional mitral regurgitation (FMR) at rest and/or its significant increase during exercise have been shown to be associated with reduced functional capacity, pulmonary oedema and impaired prognosis. [6, 49, 61, 114, 115] Only Ennezat concludes that exercise Doppler echocardiography does not refine predictive value of resting Doppler echocardiography in patients with systolic heart failure and FMR at rest. [116] In these studies, FMR has been assessed using 2-dimensional (D) quantitative techniques: proximal isovelocity surface (PISA) and pulsed Doppler volumetry. These methods, however, have several known limitations such as geometric assumptions of a hemispherical regular effective regurgitant orifice (ERO), underestimation of ERO in FMR, low reproducibility and indirect measurement of ERO. [76, 102, 104, 117] Recently, colour Doppler 3-D echocardiography-derived vena contracta cross-sectional area (VCA) has emerged as a new method to assess FMR severity at rest, which allows direct assessment of ERO without geometric and flow assumptions.[79, 82, 101-104] VCA at rest has been shown to have a higher correlation with the 2-D integrative method or magnetic resonance-derived regurgitant volume than any single 2-D method.[102, 104] However, an identification of resting predictors of exercise-induced severe FMR tracked by VCA analysis and the prognostic significance of VCA at rest and its increase during exercise has not been investigated.

Therefore, we wanted to test following hypotheses:

Secondary:

1) The relationship between exercise-induced changes of FMR assessed by VCA, clinical and Doppler characteristics is different from those described by 2D-PISA methods previously.
2) There are resting predictors of exercise-induced changes in FMR assessed by VCA.
3) There is a difference between VCA and PISA methods for assessing FMR at rest and during exercise.

Primary:

4) VCA at rest and its increase during exercise is an independent predictor of clinical outcome in our population.

6.2. Methods and patient population

The subject group consisted of 78 consecutive patients (age, 67±12 years; 78% male) with chronic systolic heart failure who were admitted for acute worsening if they fulfilled the following criteria: (1) left ventricular (LV) systolic dysfunction (LV ejection fraction <45%) of ischemic or non-ischemic origin; (2) mild-moderate FMR (<2+/4) at rest on 2-D integrative approach; [102, 104] and (3) optimal pharmacological therapy. Patients were in NYHA class I (13%), II (60%), III (27%). Ischemic origin of cardiomyopathy in 52%, arterial hypertension 48%, diabetes mellitus 27%, atrial fibrillation 34%, resynchronisation therapy 17%,. Medication used: ACEi 89%, betablockers 76%, spironolactone 75%, diuretics 87%. Subjects with VCA increase ≥ 20 cm2 in peak exercise were called MR increase group (n=24, 34%) and patients with no or less increase of VCA were called MR stable group (n=47, 66%). Patients who were unable to perform semi-supine exercise, who had acute coronary syndrome in the previous 30 days, concomitant organic mitral valve lesions or significant aortic valve disease were excluded. The study complied with the Declaration of Helsinki. The study protocol was approved by the Ethics Committees of both participating institutions. All patients gave written informed consent before inclusion in the study.

6.3. Study Protocol

After compensation, before discharge, all patients underwent resting and graded, symptom-limited exercise echocardiography using a tilting bicycle table allowing continuous echocardiography (Figure 0) monitoring in a semi-supine position. The initial workload of 25W was increased every 2min by 25W. When patient became symptomatic we did not further increase the power load but rather kept the patient cycling for at least 2 minutes. Blood pressure and 12-lead electrocardiography were recorded every 2min. 2-, 3-D and Doppler echocardiography was performed at rest and throughout the exercise. The blood sample for N-terminal of the pro-hormone B-type natriuretic peptide (NT-proBNP) was collected prior to echocardiography. In addition, right heart catheterization was performed during index hospitalization to assess invasive hemodynamic parameters in 63% of patients. Thereafter, patients were followed up clinically in our institution or by local cardiologist with the follow-up control for the prognostical part of the study within at least one year after the study enrolment. Study endpoints defined as the death of any cause, admission for the worsening heart failure or heart transplantation.

Figure 0. Tilt-able bicycle ergometer. Patient may be tilted on the left side and backwards in the position, which is almost identical with the common one, for the standard transthoracic echocardiography, resulting in almost all patients in reasonable image acquisition. (Dr.Večeřa)

6.4. Echocardiography

All echocardiography was done using a commercially available system (Vivid E9; GE Medical Systems, Horten, Norway) equipped with speckle tracking and 3-D colour Doppler imaging. All images were stored in digital format for offline analysis. The mean from at least 3 consecutive beats (5 in atrial fibrillation) was taken for each measurement both at rest and during exercise. Standard assessment of LV dimensions, LV volumes and ejection fraction (bi-apical Simpson method), sphericity index, left atrial volume (bi-apical area-length method) was performed according to the current recommendations.[118]

Electromechanical dyssynchrony between the papillary muscles was assessed using speckle tracking. In brief, in 3 apical views (4-, 3- and 2-chamber), the longitudinal strain curve was extracted from the grey scale images using dedicated software (EchoPack for PC, GE). The time interval between the beginning of the QRS complex on surface ECG and the peak of segmental contraction on the strain curve (time to peak) was analysed in the mid-ventricular segments adjacent to the papillary muscles. The peak was defined as the lowest point of the strain curve. Electromechanical dyssynchrony was defined as the difference between time to peak in the two segments adjacent to the papillary muscles.

Apical rocking is a new marker to assess LV dyssynchrony and predict CRT response. [119] It is defined as an integrative surrogate of both temporal and functional inhomogeneities within the left ventricle which may be assessed visually with reasonable accuracy. [120, 121]

Mitral Valve Deformation This was assessed in the apical 4-chamber view. The mitral valve tenting area, coaptation height, anterior and posterior mitral leaflet angle were assessed at mid-systole. Mitral annulus diameter was measured in end-diastole.

6.5. Quantification of FMR

In the apical 4-chamber view, full-volume, colon Doppler 3-D loops were recorded during respiration using the 3V-D active matrix 4-D volume phased array probe using real-time, single beat acquisition. The narrowest sector possible was used to maximize the frame rate. The average frame rate for the 3-D colour Doppler data set acquisition was 15 ± 1.8 frames/s. This frame rate provides 7–8 frames per systole at a heart rate of 60 beats/min and 6–7 frames per systole at a heart rate of 100 beats/min.[122] The typical colon code bar setting for the assessment of VCA is similar to the setting used for the PISA method, with baseline shift downward to the negative aliasing velocity between 20 and 40cm/s. The 3-D colour Doppler datasets were analysed using dedicated software (EchoPac for PC, GE) as follows: 3-D colour Doppler signals were optimized to distinguish the vena contracta from the proximal flow convergence and a rapidly expanding jet in 2 simultaneous 2D-derived perpendicular planes to ensure the best reproducibility. To identify VCA, the 3-D dataset was rotated to bisect the regurgitant colour jet at the level of leaflet coaptation zone perpendicularly to its long axis in 2 orthogonal planes. The image was cropped along the jet direction to visualize the cross-sectional area at the level of vena contracta. The VCA was defined as the high-velocity core of the colour spectrum and to avoid the “colour bleeding”, that is, the low-velocity flow signal in the periphery of the colour spectrum. To facilitate delineation of the VCA, the colour gain was lowered. In contrast to low-velocity peripheral flows, the vena contracta flow is less affected by the colour gain adjustments. When reducing gain, the high intense core of the high-velocity vena contracta flow is the last to remain.

Figure 1 shows examples of the vena contracta flow and low-velocity peripheral flows with the colour-code bar setting. The VCA at the closest frame preceding mid-systole was magnified and traced manually. Usually, this was the third or fourth systolic frame at rest and the third systolic frame during peak exercise. Furthermore, 3-D colour Doppler echocardiography-derived vena contracta cross-section length (VCL) was assessed as the largest diameter of VCA. In the case of multiple jets, VCA and VCL were calculated as the sum of the individual VCA and VCL. We may observe representative VCA tracing in 2 patients with mild-moderate FMR at rest, one with a significant exercise-induced increase of VCA (Figures 1A,B) and the other with a stable small VCA during exercise (Figures 1C,D). The 2D-derived assessments of FMR included the PISA method-derived ERO and vena contracta width. [102, 104]

PISA Method

Proximal flow convergence was acquired from magnified apical 4-chamber, 2-chamber and long-axis views, with baseline shift of the Nyquist limit (26-40 cm/s) to optimize visualization of flow convergence. Radius of the PISA was measured in the same time interval or as close as possible to timing of the VCA from the QRS onset. The ROA was calculated using the standard formula ROA=2∏RPISA² Valiasing/Vmax, where RPISA was the maximal PISA radius (cm). Valiasing was aliasing velocity of the proximal flow convergence (cm/s), and V max was maximal velocity of continuous wave Doppler MR signal (cm/s). MR volume was calculated as (ROA regurgitant time-velocity integral). The severity of MR was graded on the basis of current recommendation as mild (0,2cm²), moderate (0,2-0,39cm²), or severe (≥ 0,4cm²).

Vena Contracta Width

The vena contracta was acquired from magnified parasternal long-axis view with the central beam through the leaflet tips. Vena contracta width (VCW) was defined as the narrowest width of the proximal jet measured at or in the immediate vicinity of the MR orifice at the leaflet tips. The severity of MR was graded on the basis of current recommendation as mild (≤ 0,3cm), moderate (0,3-0,69cm) and severe (0,7cm).

Jet area to Left Atrial Area ratio

The colour flow Doppler image of the MR jet was acquired from the apical 4- and 2-chamber views at Nyquist limit of 50-60cm/s. The ratio of MR jet area to left atrial area (JA/LAA) was calculated as average from both views. The severity of MR was graded on the basis of current recommendation as mild (≤ 20%), moderate (20-39%) and severe (40%).

Two dimensional Integrative method

The two-dimensional integrative method recommended by ASE was used as the reference standard for MR grading because this method does not rely on only one colour Doppler method and is used widely in clinical laboratories. To categorize MR within a certain grade, at least 2 of 3 colour Doppler methods listed above were assessed within the same grade with at least 1 supportive data (pulmonary vein flow, mitral inflow, density of continuous wave Doppler jet, left atrial enlargement). The integrative grading and 3D VCA measurement were performed independently and the results were blinded to each other.

Figure 1 An individual example of a significant exercise-induced increase of VCA (1A, 1B) versus stable small VCA (1C, 1D). VCA (white ellipse) was assessed using manual planimetry at the closest frame preceding mid-systole. Care was taken to circle the central area of the high-velocity flow while avoiding the low-velocity colour flow signals at the periphery. VCL was measured as the maximal VCA diameter. In this patient (1A), a relatively large ellipsoid VCA was observed at rest (1A) despite the small colour-coded regurgitant jet area (right panel) and "mild" appearance of FMR. Figure 1B shows a significant increase in VCA corresponding to significant FMR during low-load exercise (50 W). It is noteworthy, that the PISA-derived ERO (1B, green circle) showed smaller increase suggesting an underestimation of ERO by the PISA method. Figure 1C and 1D show an example of a patient with the small circular VCA both at rest and during exercise, respectively, reflecting stable mild-to-moderate FMR. (Dr.Večeřa, with permission)

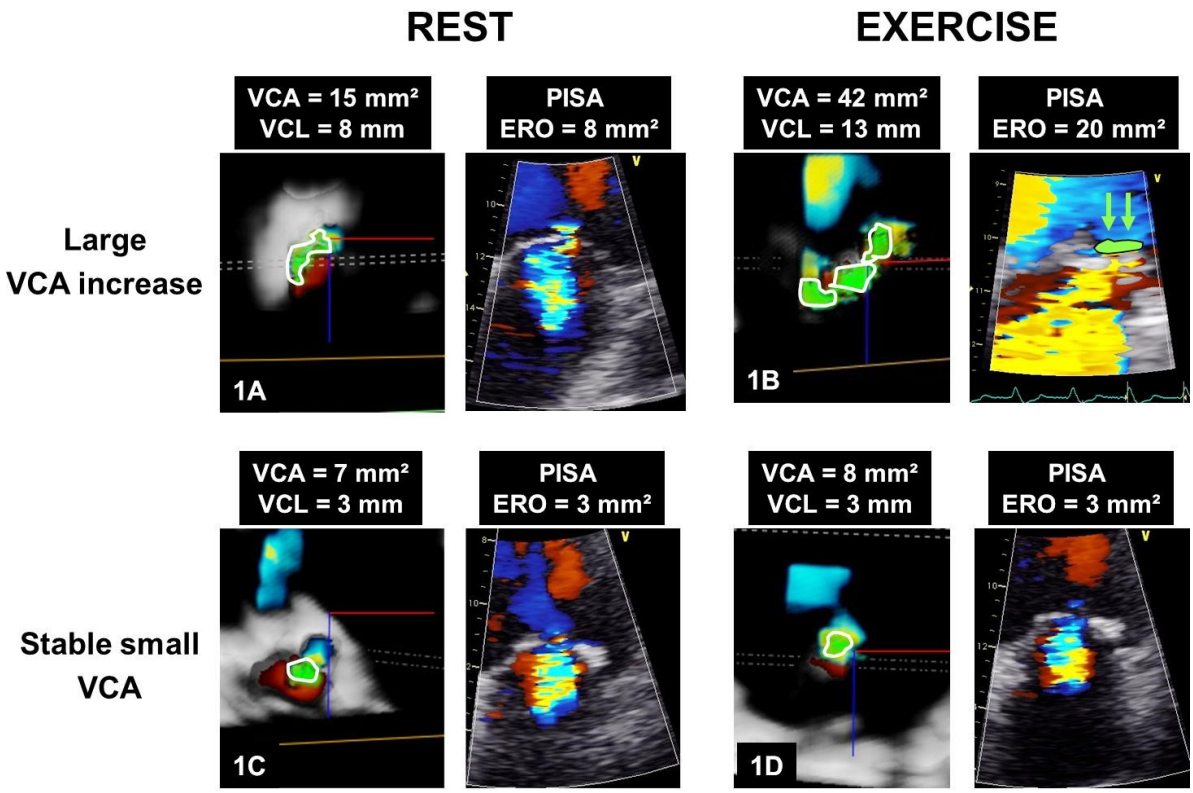

6.6. Statistical analysis

Data are presented as means for continuous variables and as percentage for categorical variables. The unpaired or paired Student´s t-test and the Pearson correlation coefficient were used as appropriate. Fisher´s exact test was used to compare categorical variables in 2x2 contingency tables.

Receiver operating characteristics curves were constructed to assess optimal cut-off for the VCA to predict clinical outcome and also to compare VCA, VCL and PISA- derived ERO. The endpoint was defined as a composite of death from any cause, admission for worsening heart failure and heart transplantation. Independent predictors of the composite endpoint were identified using Cox proportional hazard model and expressed as a hazard ratio and 95% confidence interval.

Cumulative survival curves were derived according to the Kaplan-Meier method, and differences between curves were analysed on log-rank statistics. For all tests, P<0,05 was considered significant.

6.7. Results

Seven patients (9%) had poor echocardiography image quality at rest and were excluded prior to exercise. In all of the remaining 71 patients (age 67±12 years; 79% male, LV ejection fraction 28±9%) the assessment of VCA was feasible both at rest and during exercise (feasibility, 91%). The image post-processing time to obtain VCA was 3,8±1,2 min. At peak exercise, a total of 24 (34%) patients showed a significant increase (≥20mm2) of VCA (FMR increase group). The remaining 47 (66%) individuals showed no change (n=12, 17%), mild (< 20mm2) increase (n=25, 35%) or decrease (n=10, 14%) of VCA (FMR stable group) (Figure II). Reversible ischemia was not observed with any of the patients.

For the prognostic part of the study, we had to exclude 9 patients who underwent implantation of biventricular pacemaker during index hospitalisation, because the procedure itself has a significant impact in patient´s prognosis and dynamic mitral valve behaviour. Therefore, the remaining 62 patients (age 68±11 years, 76% male) were included in the clinical outcome analysis. During a median follow-up of 17 months (IQR, 13-20 months), 15 patients (24%) reached the composite endpoint (death, n=3, admission for the worsening heart failure, n=11, heart transplantation, n=1). Follow-up was obtained with all patients.

6.7.1. Baseline and Exercise Characteristics

At baseline, the FMR increase as compared to the FMR stable group showed more advanced heart failure as documented by higher prevalence of NYHA class III (54% vs. 11%, p<0,0001), higher NT-proBNP (4971 ± 4862 pg/ml vs. 2295 ± 3245 pg/ml, p=0,0094), higher left atrial volume (62 ± 26 ml/m2 vs 48 ± 14 ml/m2, p=0,0038), while the prevalence of cardiac resynchronisation therapy, atrial fibrillation or ischemic cardiomyopathy was similar in both groups. Patients in FMR increase group were more often and more frequently hospitalized for acute heart failure (67% vs. 26%, p= 0,0017; 29% vs. 4%, p= 0,0055). Hospitalization for pulmonary oedema was observed only in FMR increase group (25% vs. 0%, p=0,0006).

In terms of LV morphology, systolic function, mitral valve architecture and invasively measured PCW pressure and mPA pressures showed also no significant difference. Of note, the PISA method-derived ERO (10 ± 4mm2 vs. 9 ± 7mm2, NS) was similar in both groups. In contrast, the FMR increase group showed significantly larger VCA (17±6mm2 vs. 12±7mm2, p<0,0019) and 3D derived VCL (7,6±2,1mm vs. 4,5±2,4mm, p<0,0001), larger electromechanical dyssynchrony between the papillary muscles reflected by longitudinal strain peak difference (144±128ms vs. 69±56ms, p=0,001) compared with FMR stable group. We also observed significantly higher incidence of apical rocking (38% vs. 6%, p=0,0018) and more often severely impaired systolic function of the segment adjacent to the postero-lateral papillary muscle (46% vs. 6%, p=0,0002) (Table I).

Table I. Baseline clinical, echocardiography and hemodynamic characteristics – whole group

	FMR increase n = 24	FMR stable n = 47	P value
Age, years	70.4 ± 10.1	66.0 ± 12.1	0.14
Sex, % females	26	19	1.0
Diabetes mellitus, n (%)	9 (38)	10 (21)	0.17
Coronary artery disease, n (%)	11 (46)	26 (55)	0.47

ACE inhibitors, n %	21 (88)	42 (89)	1.0
Beta-blockers, n (%)	21 (88)	33 (71)	0.15
Spironolactone, n (%)	19 (79)	34 (74)	0.77
Loop diuretics, n (%)	22 (91)	40 (85)	0.71
NYHA III, n (%)	13 (54)	5 (11)	< 0.001
NT proBNP, pg/ml	4971 ± 4862	2295 ± 3245	0.009
Hospitalization for worsening HF in preceding 2 years, n (%)	16 (67)	12 (26)	0.002
≥ 2 hospitalizations for worsening HF in preceding 2 years, n (%)	7 (29)	2 (4)	0.006
Pulmonary edema in the preceding 2 years, n (%)	6 (25)	0 (0)	< 0.001
Glomerular filtration rate, ml/min	58 ± 19	63 ± 15	0.21
Atrial fibrillation, n (%)	12 (50)	12 (26)	0.06
QRS width, ms	141 ± 31	128 ± 34	0.17
CRT, n (%)	6 (25)	6 (13)	0.31
LV ejection fraction, %	25 ± 7	29 ± 8	0.09
Mitral regurgitation moderate, %			
LA volume index, ml/m²	62 ± 26	48± 14	0.004
PPM dyssynchrony, ms	144 ± 128	69 ± 56	0.001
PPM adjacent segment severe WMA, %	11 (46)	3 (6)	< 0.001
Apical rocking, n (%)	9 (38)	3 (6)	0.002
Mean PAP, mmHg	28 ± 9	24 ± 9	0,.15

PCWP, mmHg	21 ± 9	17 ± 7	0.11
Cardiac index, l / min / m²	2.2 ± 0.6	2.3 ± 0.6	0.96

Abbreviations: CRT = cardiac resynchronization therapy, FMR = functional mitral regurgitation, HF = heart failure, LA = left atrium, PAP = pulmonary artery pressure, PCWP = pulmonary capillary wedge pressure, PPM = papillary muscles, WMA = wall motion abnormality

Exercise characteristics

The FMR increase group showed significantly lower peak exercise load (50±24W vs. 86±36W, p<0,0001), higher systolic pulmonary artery pressure (53±8 mmHg vs. 43±10mmHg, p=0,002). We observed significantly lower end-diastolic left ventricular sphericity index during exercise in FMR increase group. Concerning mitral valve architecture there was also higher tenting area (2,7±1,1cm2 vs 1,7±0,7cm2, p=0,0001), higher coaptation height (10,4±4,0 mm vs. 7,0±2,4mm, p <0,0001) and significantly higher posterior leaflet angle (PLA) (34±12 dg. vs. 25±9 dg., p=0,024), anterior leaflet angle 32±17 dg. v.s. 20±9 dg., p=0,024) compared with the FMR stable group. Furthermore, at peak exercise, the FMR increase compared to stable group showed significantly larger VCA (42±7mm2 vs. 15±8mm2, p<0,0001) and PISA-derived ERO (24 ±7 mm2 vs. 12±9 mm2, p<0,0001). Of note, the rest to peak exercise differences of PISA-derived ERO were significantly lower than differences in VCA (6±8 mm2vs. 11±13mm2, p=0,0227). The exercise induced significant increase of PISA derived ERO (>13mm2) identified only 14 out of 24 (58%) of patients with significant increase of VCA (>20mm2), which may suggest lower sensitivity of PISA method. (Table II, table III)

Table II. Selected indices of LV remodeling and mitral valve deformation at rest and during exercise

	FMR increase n = 24	FMR stable n = 47	P value
Exercise tolerance, Watts	50 ± 24	86 ± 36	< 0.001
Heart rate, bpm			
Rest	73 ± 15	71 ± 17	0.84
Exe	97 ± 22 ‡	104 ± 26 ‡	0.28
Systolic blood pressure, mmHg			
Rest	113 ± 17	115 ± 20	0.17
Exe	133 ± 23 ‡	143 ± 27 ‡	0.06
Peak TR gradient, mmHg			
Rest	21 ± 7	21 ± 6	0.64
Exe	53 ± 8 ‡	43 ± 10 ‡	0.002
LV end-diastolic volume index, ml / m^2			
Rest	104 ± 47	91 ± 26	0.13
Exe	112 ± 46	91 ± 29	0.03
LV end-systolic volume index, ml / m^2			
Rest	79 ± 41	66 ± 24	0.09
Exe	83 ± 43	62 ± 26 †	0.02
LV ejection fraction, %			
Rest	25 ± 7	29 ± 8	0.09

Exe	28 ± 8	33 ± 11 ‡	0.06
LV sphericity index			
Rest	1.53 ± 0.18	1.57 ± 0.21	0.43
Exe	1.47 ± 0.17	1.58 ± 0.21	0.04
Mitral annulus diameter, mm			
Rest	42.3 ± 5.1	42.3 ± 4.2	0.97
Exe	42.8 ± 4.3	42.0 ± 3.6	0.46
Mitral valve tenting area, cm^2			
Rest	1.8 ± 1.0	1.6 ± 0.7	0.37
Exe	2.7 ± 1.1 ‡	1.7 ± 0.7	< 0.001
Mitral valve coaptation height, mm			
Rest	8.0 ± 3.6	6.8 ± 2.6	0.11
Exe	10.4 ± 4.0 †	7.0 ± 2.4	< 0.001
Anterior leaflet angle, degrees			
Rest	22 ± 12	18 ± 10	0.21
Exe	32 ± 17 †	20 ± 9	< 0.001
Posterior leaflet angle, degrees			
Rest	27 ± 11	25 ± 9	0.37
Exe	34 ± 12 †	25 ± 9	< 0.001

∗ $p < 0.05$, † $p < 0.01$, ‡ $p < 0.001$ rest versus exercise

Out of the 24 patients with significant (≥ 20mm^2) increase in VCA only 14 (58 %) ones had significant (≥13mm^2) increase of the PISA-derived ERO. A subgroup of patients, in whom the PISA method failed to identify an exercise-induced significant FMR indicated by VCA rise (≥ 20mm^2, showed at rest and during exercise significantly higher PLA (33±0 dg. vs. 23±11 dg., p=0,04; 41±7 dg. vs. 29±13 dg., p=0,011) and coaptation height (9,8±3,9mm vs 6,8±2,9mm, p=0,04; 12,5±3,3mm vs 8,9±3,0mm, p=0,03) than patients in whom PISA correctly identified exercise induced FMR (Table VI). In contrast, both subgroups had similar global echocardiography characteristics and VCA at peak exercise and patients in PISA failure group reached significantly lower PISA derived ERO (18±5mm2 vs. 27±6mm2, p=0,0004) while on the contrary VCA (40±7mm2 vs. 44±6mm2, p=0,16). Of note, the exercise capacity was similar in the both PISA subgroups but significantly lower than in patients without an exercise-induced increase in VCA.

Table III. Three- and two-dimensional derived Doppler echocardiography indices to assess FMR at rest and during exercise

	FMR increase n = 24	FMR stable n = 47	P value
Integrative approach FMR quantification,			
% moderate FMR (at rest),	63	38	0,07
% moderate and severe FMR (exercise)	100	45	< 0.001
Vena contracta length (3D), mm			
Rest	7.6 ± 2.1	4.5 ± 2.4	< 0.001
Exe	15.4 ± 2.9 ‡	6.1 ± 3.2 †	< 0.001
Vena contracta area (3D), mm^2			
Rest	17 ± 6	12 ± 7	0.002

Exe	42 ± 7 ‡	16 ± 8 †	< 0.001
Effective regurgitant orifice (2D PISA), mm^2			
Rest	10 ± 4	9 ± 7	0.34
Exe	24 ± 7 ‡	12 ± 9 ‡	< 0.001
Vena contracta (2D), mm			
Rest	3.5 ± 1.0	2.7 ± 1.3	0.02
Exe	6.4 ± 1.2 ‡	3.1 ± 1.3	< 0.001
Regurgitant jet area / left atrial area (2D)			
Rest	13 ± 5	10 ± 8	0.15
Exe	26 ± 13 ‡	15 ± 11 ∗	< 0.001
≥ 2 regurgitant jets (2D), %			
Rest	11 (46)	10 (21)	0.05
Exe	8 (33)	9 (19)	0.24

∗ $p < 0.05$, † $p < 0.01$, ‡ $p < 0.001$ rest versus exercise

Abbreviations: 2D = two-dimensional, 3D = three dimensional

6.7.2. Resting predictors of the exercise-induced increase in FMR

Resting VCL ≥ 7mm showed the best ability (AUC=0,84, sensitivity 83%, specificity 77%) to identify patients with significant exercise-induced FMR. The electromechanical dyssynchrony ≥ 60ms between the papillary muscles showed lower accuracy (AUC = 0,69, sensitivity 71%, specificity 77%) for the peak contraction. VCA ≥ 17mm2 gave us also reasonable predictive value (AUC = 0,74, sensitivity 58%, specificity 79%). Left ventricle apical rocking was significantly more often observed in FMR increase group (38% vs 6%, p= 0,0018). Significantly more impaired function of the LV segment adjacent to the anterolateral papillary muscle (akinetic or severely hypokinetic) was also significantly more often observed in FMR increase group (38% vs. 6%,p= 0,0018). When combined apical rocking and/or impaired anterolateral papillary muscle dysfunction showed accurate predictive values for FMRi with sensitivity 71%, specificity 87%, PPV 74%, NPV 85%.

Large VCA and small PISA-derived ERO during peak exercise This analysis included all 71 patients age 67±12 years, 79% males) with good image quality both at rest and during exercise. Out of the 24 patients with significant (≥ 20mm^2) increase in VCA only 14 (58 %) ones had significant (≥13mm^2) increase of the PISA-derived ERO. Subgroup of patients, in whom the PISA method failed to identify an exercise-induced significant FMR, showed significantly higher coaptation height and posterior leaflet angle at rest and during exercise than patients in whom PISA correctly identified exercise induced FMR (Table VII). In contrast, both subgroups had similar global echocardiography characteristics and VCA at peak exercise. Of note, the exercise capacity was similar in the both PISA subgroups but significantly lower than in patients without an exercise-induced increase in VCA.

Table VII. Echocardiography characteristic of patients with large exercise-induced increase in VCA (≥ 20 mm²) and with consistent large (≥ 13 mm²) versus discrepant small (< 13 mm²) increase in the PISA-derived ERO.

VCA increase (≥20mm2) (n=24)	PISA ERO increase (≥ 13 mm²), N=14	PISA ERO increase (< 13 mm²), N=10	P-value

Effective regurgitant orifice (2D PISA) mm^2			
Rest	10 ± 4	11 ± 4	0.4
Exe	27 ± 6 ‡	18 ± 5 ‡	< 0.001
Vena contracta area (3D), mm^2			
Rest	17 ± 6	18 ± 5	0.91
Exe	44 ± 6 ‡	40 ± 7 ‡	0.16
LV end-diastolic volume index, ml / m^2			
Rest	95 ± 29	117 ± 66	0.29
Exe	104 ± 31	122 ± 61	0.37
LV end-systolic volume index, ml / m^2			
Rest	70 ± 27	91 ± 55	0.25
Exe	74 ± 32	92 ± 55	0.38
LV ejection fraction, %			
Rest	27 ± 7	23 ± 6	0.18
Exe	29 ± 10	27 ± 7	0.44
LV sphericity index			
Rest	1.56 ± 0.13	1.50 ± 0.23	0.45
Exe	1.46 ± 0.18°	1.50 ± 0.16	0.58
Mitral valve tenting area, cm^2			
Rest	1.6 ± 0.7	2.2 ± 1.2	0.15
Exe	2.4 ± 1.0 ‡	3.2 ± 1.3 ‡	0.11
Mitral valve coaptation height, mm			
Rest	6.8 ± 2.9	9.8 ± 3.9	0.04

Exe	8.9 ± 3.9 †	12.5 ± 3.3 ‡	0.03
Anterior leaflet angle, degrees			
Rest	19 ± 10	27 ± 14	0.1
Exe	27 ± 11 ‡	35 ± 13	0.12
Posterior leaflet angle, degrees			
Rest	23± 11	33 ± 9	0.04
Exe	29 ±13 ∗	41 ± 7 ‡	0.011
Exercise capacity, Watt	46 ± 19	55 ± 31	0.41

∗ $p < 0.05$, † $p < 0.01$, ‡ $p < 0.001$ rest versus exercise

Abbreviations as in the previous table

6.7.3. Prognostic group baseline characteristics

At baseline, patients with endpoint compared to patients without endpoint had more advanced heart failure as evidenced by significantly higher NT-proBNP, wider QRS complex and reduced tricuspid annular plane systolic excursion (all P<0,05;Table IV). Moreover, in the two years preceding the study inclusion, patients with endpoint were more likely to be admitted repeatedly for worsening heart failure (P<0,001) than individuals without endpoint. Prevalence of cardiac resynchronisation therapy, ischemic cardiomyopathy or atrial fibrillation was simile in both Gross. E/e´, degree of global remodelling and ejection fraction, and the indices of mitral valve deformation did not differ between groups (Table IV). Furthermore, the endpoint group had a significantly larger VCA (P=0,002), VCL (P=0,02) and higher prevalence of large (≤20mm²) ´ prognostic´ VCA (P=0,02) at rest than patients without the endpoint. (Table V) In contrast, out of the 2D –derived indices, only PISA method-derived ERO tended to be larger (P=0,06) in patients with versus without endpoint, while the vena contracta width was similar. No patient had prognostic PISA derived ERO (≤20mm²). At peak exercise, the endpoint group had a significantly lower peak exercise load and systolic blood pressure (both P<0,01) compared with the group without endpoint. Reversible myocardial ischemia was not observed in any of the patients. The indices of LV remodelling and ejection fraction were similar. Both groups had significant rest-to exercise increase in VCA, VCL, PISA-derived ERO and vena contracta width (all P<0,01); but significantly larger VCA, VCL and vena contracta width (all P<0,01), and slightly larger PISA-derived ERO (P=0,07) were observed in the endpoint group. (Table V)

Table IV. Baseline clinical and echocardiography characteristics – prognostic part

	+ ENDPOINT n = 15	- ENDPOINT n = 47	P value
Age, years	65 ± 16	68 ± 9	0.36

Sex, % females	20	17	1.0
Diabetes mellitus, n (%)	4 (27)	11 (23)	1.0
Coronary artery disease, n (%)	9 (60)	25 (53)	0.77
ACE/ATII inhibitors, n %	14 (97)	44 (94)	1.0
Beta-blockers, n (%)	12 (80)	33 (72)	0.74
Spironolactone, n (%)	12 (80)	30 (64)	0.35
Loop diuretics, n (%)	14 (97)	36 (76)	0.26
NYHA class	2.5 ± 0.5	2.0±0.6	0.09
NT proBNP, pg/ml	5034 ± 5196	2524 ± 3556	0.038
Hospitalization for worsening HF in preceding 2 years, n (%)	12 (80)	20 (43)	0.017
≥ 2 hospitalizations for worsening HF in preceding 2 years, n (%)	8 (53)	2 (4)	< 0.0001
Glomerular filtration rate, ml/min	61 ± 19	60 ± 14	0.95
Atrial fibrillation, n (%)	7 (47)	16 (34)	0.54
QRS width, ms	143 ± 33	123 ± 33	0.031
CRT, n (%)	4 (27)	5 (11)	0.2
TAPSE, mm	15.5 ± 3.1	17.8 ± 4.0	0,047
LA volume index, ml/m²	55 ± 18	51 ± 22	0.52

Abbreviations: CRT = cardiac resynchronization therapy, HF = heart failure, LA = left atrium, TAPSE = tricuspid annular plane systolic excursion

Table V. Selected 2D and 3D derived Doppler echocardiography indices at rest and during exercise

	+ ENDPOINT n = 15	- ENDPOINT n = 47	P value
Exercise tolerance, Watts	52 ± 20	81 ± 38	0.007
Heart rate, bpm			
Rest	69 ± 16	72 ± 15	0.55
Exe	96 ± 27 ‡	103 ± 23 ‡	0.38
Systolic blood pressure, mmHg			
Rest	105 ± 17	118 ± 19	0.021
Exe	126 ± 20 ‡	146 ± 23 ‡	0.004
LV end-diastolic volume index, ml / m^2			
Rest	102 ± 54	90 ± 24	0.25
Exe	109 ± 18	90 ± 26	0.06
LV end-systolic volume index, ml / m^2			
Rest	75 ± 47	64 ± 19	0.62
Exe	78 ± 22	60 ± 27 †	0.08
LV ejection fraction, %			
Rest	29 ± 8	29 ± 8	0.46
Exe	30 ± 8	33 ± 10 ‡	0.12
LV sphericity index			
Rest	1.52 ± 0.17	1.52 ± 0.16	0.32

Exe	1.58 ± 0.20	1.56 ± 0.21	0.54
Peak TR gradient, mmHg			
Rest	21 ± 7	23 ± 6	0.42
Exe	50 ± 8 ‡	45 ± 9 ‡	0.056
Vena contracta area (3D), mm^2			
Rest	17 ± 6	13 ± 7	0.002
Exe	35 ± 16 ‡	21 ± 12 ‡	< 0.001
Rest VCA ≥ 20 mm^2, n (%)	8 (53)	10 (21)	0.02
Exe-induced VCA increase ≥ 20 mm^2, n (%)	9 (60)	9 (19)	0.007
Vena contracta length (3D), mm			
Rest	7.0 ± 2.9	5.1 ± 2.5	0.017
Exe	12.9 ± 6.7 ‡	8.1 ± 4.6 ‡	0.002
ERO (2D PISA), mm^2			
Rest	11 ± 5	8 ± 5	0.058
Exe	20 ± 9 †	14 ± 10 ‡	0.07
Rest ERO ≥ 20 mm^2, n (%)	0	0	N.A.
Exe-induced ERO increase ≥ 13 mm^2, n (%)	6 (40)	9 (19)	0.16
Vena contracta width (2D), mm			
Rest	3.3 ± 0.7	2.9 ± 1.3	0.2
Exe	5.3 ± 2.3 †	3.9 ± 1.6‡	0.008

∗ $p < 0.05$, † $p < 0.01$, ‡ $p < 0.001$ rest versus exercise

Abbreviations: 2D = two-dimensional, 3D = three dimensional, ERO = effective regurgitant orifice, VCA = vena contracta area

6.7.4. Study endpoints

List of individual endpoints in the group of patients with severe dynamic VCA : 1) heart failure decompensation together with ventricular arrhythmias followed by mitral valve plasty 2) heart failure decompensation followed by mitral valve plasty 3) heart failure progression and atrial fibrillation solved by mitral valve plasty with left atrial cryoablation, 4) heart failure decompensation and mitral regurgitation progression to sever at rest – Mitra clip was implanted, 5) sepsis, possible cause biventricular defibrillator related endocarditis, death, 6) heart failure decompensation with left ventricle systolic function deterioration leading to biventricular ICD implantation 7) heart failure progression to the end-stage heart failure with left ventricle systolic dysfunction progression leading to heart transplantation 8) heart failure decompensation 9) heart failure decompensation

List of individual endpoints in the group of patients without severe dynamic VCA: 1)) heart failure decompensation due to supraventricular tachycardias limiting CRT function 2) clinician and patient decision to undergo mitral valve plasty 3) heart failure decompensation 4) progression to the terminal heart failure and death 5) heart failure decompensation 6) progression to the terminal heart failure and death

6.7.5. Predictors of composite endpoint

Resting VCA and its increase were better predictors for the composite endpoint than PISA ERO increase (Figure II) . Resting VCA with a cut off ≥15mm² and its increase (cut off ≥20 mm²) at peak exercise had the highest accuracy for predicting the composite endpoint.

Concomitant presence of large VCA at rest and its significant increase during exercise occurred in 53% of patients with endpoint but only in 8% patients without endpoint (negative predictive value, 86%; AUC=0,76). VCL at rest (area under the curve (AUC=0.68), VCL at peak exercise (AUC=0.73) and exercise–induced increase in PISA derived ERO (AUC=0,60) had lower accuracy. On Cox regression analysis, resting VCA ≥15mm², its ≥20 mm² exercise-induced increase and VCL ≥13mm at peak exercise were identified as the only independent predictors of composite endpoint (Table VI). The patients with VCA ≥15mm² or VCA increase ≥ 20 mm² had worse prognosis on Kaplan-Meier analysis (Figure IV).

Figure II. Vena contracta area at rest, its increase during exercise and the composite endpoint. Agreement between the presence (+) or absence (-) of large (≥ 15 mm²) VCA at rest **(top)**, the presence or absence of significant exercise-induced increase (≥ 20 mm²) of VCA **(middle)**, the concomitant presence or absence of both indices **(bottom)** and the composite endpoint.

AUC = area under the curve, Sp = specificity, Ss = sensitivity

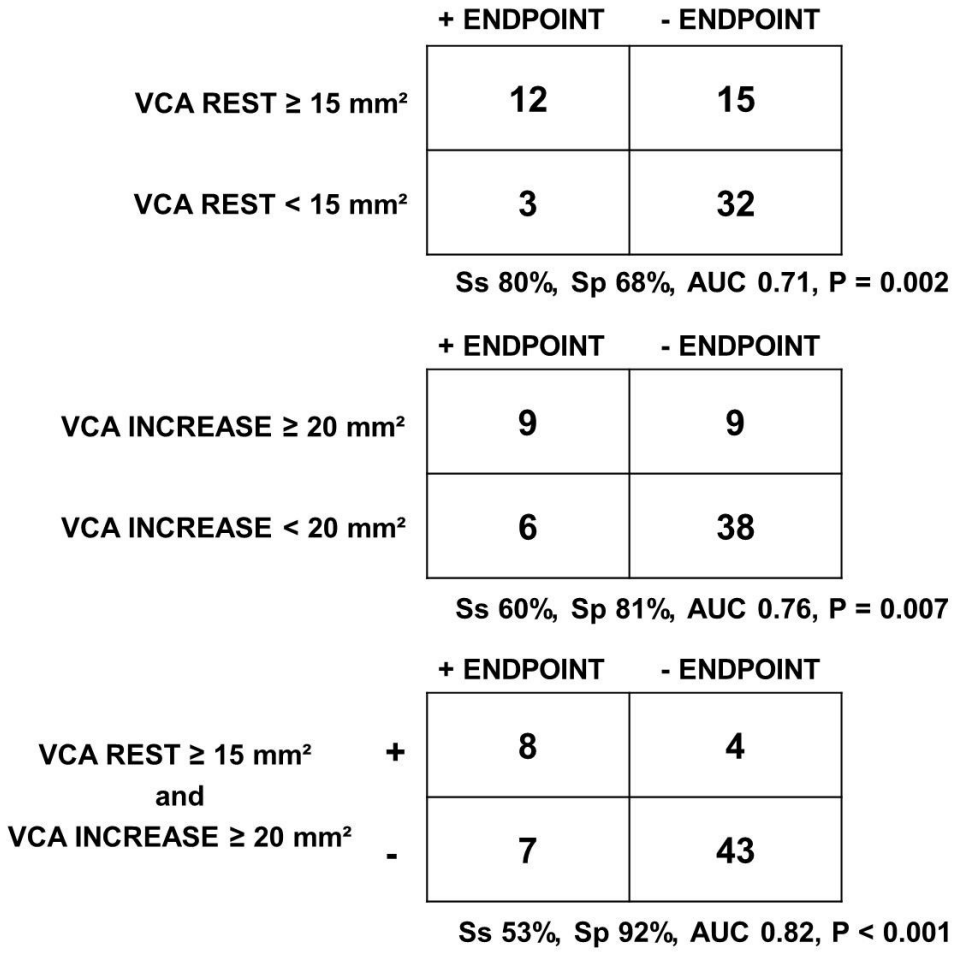

Table VI. Hazard ratio by Cox regression analysis for a composite of death from any cause or admissions for worsening heart failure or heart transplantation.

	Univariable Analysis		Multivariable Analysis	
	HR	p value	HR (95% CI)	p value
Age	0.99	0.69		
NYHA	3.1	0.024		
NT proBNP	1.0	0.07		
QRS duration	1.0	0.09		
Left ventricular ejection fraction	0.97	0.45		
TAPSE	0.86	0.054		
Exe increase PISA-derived ERO ≥ 13 mm²	1.13	0.064		
VCL at rest ≥ 7 mm	1.32	0.024	1.16 (0.86-11.89)	0.083
VCL at peak exe ≥ 13 mm	7.40	0.002	5.85 (1.67-14.09)	0.009
Resting VCA ≥ 15 mm²	8.11	<0.001	7.60 (1.93-13.02)	0.004
Exe increase VCA ≥ 20 mm²	6.33	0.004	5.10 (1.39-15.21)	0.014

CI = confidence interval, Exe = exercise, HR = hazard ratio

Abbreviations in previous tables.

2-D vs. 3D indices for Assessment of FMR

At rest, a prognostic ERO (≥ 20 mm²) was observed in 18 patients (29%) using the 3D VCA method but in no patients using the 2D PISA method (Table IV). A total of 26 patients (42%) had large 3D VCL (≥7mm) suggesting significant FMR at rest, while no patient had wide 2D vena contracta. Patients with VCA ≥20 mm² or 3D VCL (≥7mm) had higher occurrence of composite endpoint (8/15 vs. 10/47, P=0,02 for VCA or 10/15 vs. 16/47 for VCL, P=0,04 for VCL). At peak exercise a total of 18 (29%) had large (≥20 mm²) exercise induced increase in VCA and total of 15 patients (24%) had large (≥13 mm²) exercise induced increase in PISA-derived ERO. Figure IV shows VCA and PISA-derived ERO at rest and during exercise in patients with endpoint. Both VCA and PISA-derived ERO increased significantly (both p<0,01) , but rest to peak exercise difference in VCA was significantly larger than the difference in PISA derived ERO (18±10mm² vs. 9±7mm²; P<0,001; Figure IV). A significantly higher proportion of patients with endpoint had ≥20 mm² increase in VCA compared to patients without endpoint (9/15 vs. 9/47, P=0.007). In contrast, the percentage of patients with (≥13 mm²) increase in PISA derived ERO was similar between the groups (6/15 vs. 9/47, P=0,16, Table IV,V).

Figure III. Kaplan–Meier estimates of the time to death resulting from any cause, admissions for worsening heart failure or heart transplantation. Patients are divided into 2 groups according to the presence or absence of VCA ≥ 15 mm² at rest **(A)** or the presence or absence of exercise-induced increase of VCA ≥ 20 mm² at peak exercise **(B)**.

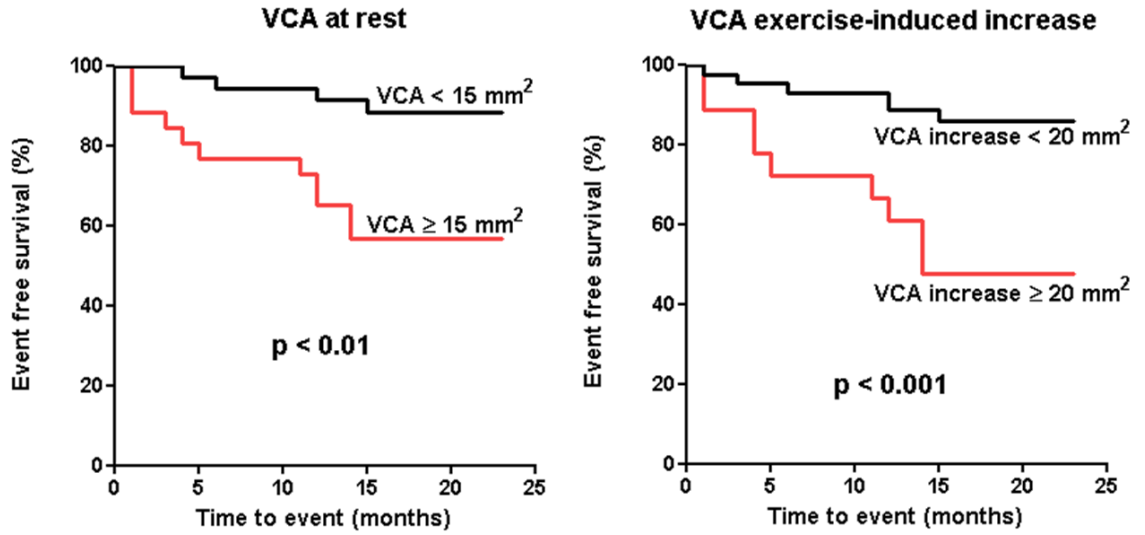

Figure IV. A comparison between the PISA-derived ERO and the three-dimensional (3D) VCA at rest and during exercise in patients with the composite endpoint.

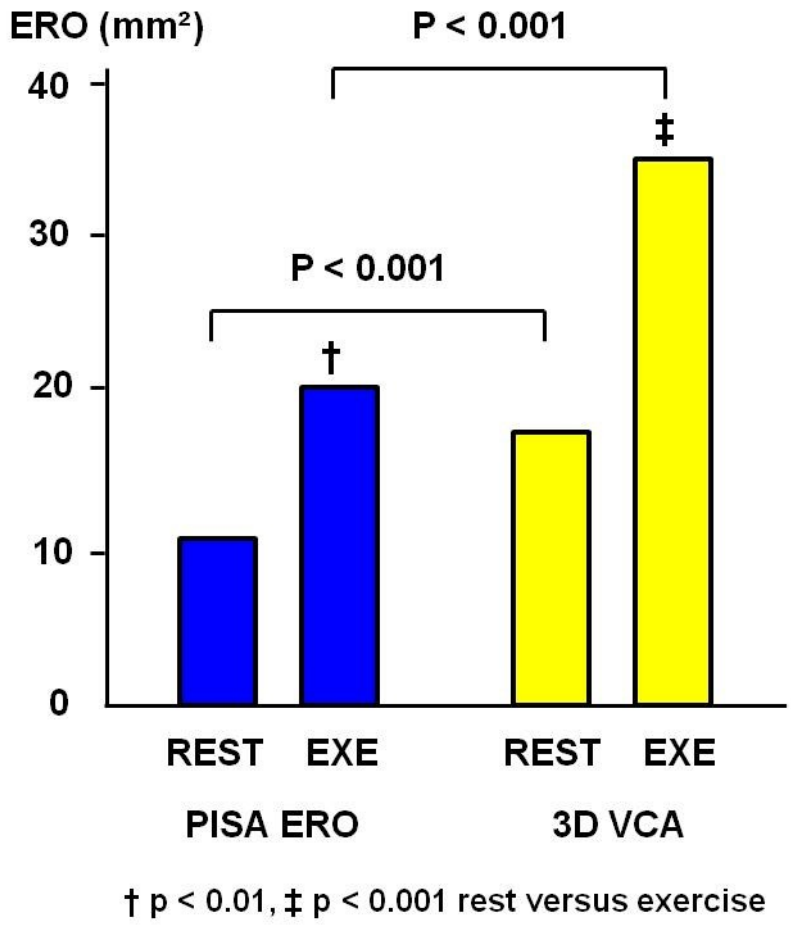

Reproducibility Reproducibility for the VCA both at rest and during exercise was assessed in 10 randomly selected patients from recorded images. Intra-observer and inter-observer variability was 7 % and 9 % at rest, and 8 % and 10 % during exercise, respectively.

6.8. Discussion

The findings of the present study can be summarized as follows:

- Although not being defined as the aim , but rather the cornerstone of the study, we would like to comment on the feasibility of assessment of VCA during bicycle exercise.
- The relationship between exercise-induced changes of FMR assessed by VCA, clinical and Doppler characteristics is not different from those described previously by PISA derived 2D methods.
- We observed that larger VCL, presence of apical rocking, as a simple marker of mechanical dyssynchrony of the left ventricle, and anterolateral papillary muscle adjacent wall motion abnormality have quite reasonable predictive value for the significant exercise induced FMR increase assessed by VCA.
- We proved that there a difference between VCA and PISA methods for assessing FMR at rest and during exercise.
- We proved that VCA at rest and its increase during exercise is an independent predictor of clinical outcome.

The VCA at rest seems to be more sensitive while its exercise induces increase seems to be more specific parameter to identify patients with the adverse clinical outcome.

Third, the assessment of VCA seems to be highly sensitive to track exercise-induced changes in FMR while the PISA method underestimates ERO both at rest and during exercise.

6.8.1. Feasibility and reproducibility

Dataset acquisition for the integrative method MR assessment method is strongly dependent on the operators experience, transducer angulation, colour Doppler adjustment especially in FMR where the shape of ERO is non-circular [78] and the operator should assess two- and four-chamber view to reveal true size of FMR.

Moreover, conventional 2D colour Doppler imaging does not provide appropriate orientation of 2D scan planes to obtain an accurate cross-sectional view of the vena contracta [98, 100] while using 3D colour Doppler acquisition the operator may easily assess proper position of the probe in mode of 2-plane simultaneous imaging and in the same position acquire 3D dataset for further analysis. Such approach may substantially decrease the time of data acquisition which is of utmost importance during exercise when dynamic changes may come and disappear very fast. Current guidelines [90] 3D TEE multiple-beat full-volume acquisition is recommended for detailed colour flow analysis, eventually 3D TTE as an alternative, to improve temporal resolution. However, in our study we used single-beat (live) 3D colour Doppler acquisition which has relatively poor spatial and temporal resolution with 14 to 17 voxel/sec. with reasonable reproducibility and as shown further on with clinical impact. There are several reasons to prefer single-beat to multiple-beat acquisition and transthoracic to transoesophageal examination, currently recommended method:

1) TEE is not usable for dynamic exercise and the severity of functional MR is affluence by current hemodynamic status which is affected by sedation usually given during TEE.
2) Multi-beat acquisition is not usable in case of irregular heart rate (atrial fibrillation, premature beats) which come frequently in patients with systolic heart failure causing stitching artefacts.
3) Breathlessness during exercise is very difficult and may affect hemodynamics especially in patients who are not able to hold the breath in calm way.

Several studies have demonstrated high feasibility and reproducibility of the VCA assessment at rest[76, 79, 82, 101, 102, 104] The current study extends these findings by showing high feasibility (91 %) and reproducibility of the VCA measurement also during low-grade exercise with a short image post-processing time bellow 5 min. The feasibility of colour Doppler 3D echocardiography-derived VCA assessment has been related to the 2D echocardiography image quality at rest. In all the patients with an acceptable 2D image quality at rest, the assessment of VCA was feasible both at rest and during exercise. Similarly, the intra- and inter-observer variability of the VCA assessment was low (< 10 %) and not significantly affected by bicycle exercise.

6.8.2. The relationship between exercise-induced changes of FMR assessed by VCA, clinical and echo-Doppler characteristics is similar to previously described using PISA derived ERO changes

Baseline differences FMR increase vs FMR stabile

There were significant differences between FMR increase and stabile group already at baseline with worse exercise capacity reflected by NYHA class, which was already observed and reflects the fact of unfavourable hemodynamic effect of exercise induced MR lowering the stroke volume. [45, 48, 123] Patients in FMR increase group were more often and more frequently hospitalised for acute heart failure and also for acute pulmonary oedema. ($p<0,01$ for all).

This finding confirms previous results of Lancellotti and Pierard [6, 59]. In patients with systolic heart failure BNP level increases with the severity of LV dysfunction and MR severity and reflects prognosis and exercise capacity in this population [124]

Higher NT-proBNP levels at rest in FMR increase group therefore reflect pronounced severity of the heart failure in this group and worse prognosis although there was no significant difference in EROs between these two groups. Such difference was not observed by Izumo 2006 EHJ [123] using BNP. We did not check dynamic behaviour of NTproBNP levels already described by Lancellotti [125]. 2D end-diastolic Sphericity index was not significantly different between groups at rest which was also observed by Lapu Bula 2002 [47], but recent work by Izumo 2009 showed that the 3D-sphericity index could identify patients with dynamic FMR at rest [44].

Among mitral valve architecture parameters there was no significant parameter to predict FMR increase which was also observed by other groups [45, 59, 123]. Lancellotti (JACC 2003) describes significant differences between tenting area and coaptation height at rest among patients with significant correlation with the MR severity, but shows no data for MR increase prediction as concerns mitral valve deformation parameters [45]

Dyssynchrony assessment

We suggested longitudinal strain analysis based parameters to assess interpapillary muscle dyssynchrony assessing electromechanical delay in peak contraction of the segments adjacent to the papillary muscle base. There was a significant difference both at rest and during exercise in FMR increase group which was not described before in this setting (p=0.001, p=0.0495.) Dyssynchrony assessment using other methods was already described before by Ennezat (EHJ 2006) who showed that changes in ERO and RV significantly correlated with the degree of LV asynchronism at rest using pulsed-wave DMI [42]. Several authors showed significant correlation of exercise induced increase in LV dyssynchrony and dynamic MR assessed by colour tissue Doppler analysis [126, 127].

Multiple jets

There were multiple, mostly, two jets in 30% of our population. Proper assessment of the MR severity in such cases reveals strong limitations while using the integrative method. 2D colour Doppler views show only one MR jet properly at one time and bicomisural view in these cases does not always allow correct measurement of VC or PISA radius. There is also a tendency to overestimate the true MR severity especially when jets are eccentric showing confluence. Such trend was confirmed by Lin BA (JASE 2010) using in vitro model where colour Doppler jet area was not appropriate for MR severity assessment with 62% overestimation compared to comparable single jet MR. [128] Addition of EROA of several jets is not recommended in current guidelines due to limited ability of 2D methods to precisely measure ERO in multiple jets. [3] However, it is logical to sum up all regurgitant jets to get true MR severity and we used such concept in our study.

Exercise related changes

Patients with FMRi achieved lower cycle work rate (50±24W vs 84±29W, p<0,0001) reflecting lower exercise capacity which correlates with previous findings [48, 129].

During exercise, there was a significant difference in enddiastolic and endsystolic volume index between FMRI and FMRS groups (p=0,026, p=0,02) probably reflect volume overload adaptation and was already observed. [129]

There were significant exercise – induced changes in LV shape in FMRi group showing increasing sphericity of the left ventricle which was not observed in FMRS group (p<0,0001). Such deformation probably contributes secondary to the mitral valve apparatus deformation and dynamic increase of the FMR which was also observed by Izumo group. [44]

All leaflets angles reflecting mitral valve deformation were significantly higher during exercise in FMRi group increased (p<0,001) and such finding was already observed. [44, 47]

Significant difference increase in TI gradient reflecting higher pulmonary artery pressure was observed in concordance with previous studies. [59]

6.8.3. The behaviour of the FMR during exercise prediction

Currently, the most challenging task is to differentiate moderate to severe MR in terms of morbidity, mortality and mitral valve surgery timing. [61, 115, 130, 131]

We assume that mild MR assessment may reveal significant and clinically relevant differences. PISA method failed to show difference between both groups at rest but 3D VCA analysis revealed multiple jets in one third of the patients and significantly higher VCA and VCL in FMR increase group. Such finding may reflect the fact that precise assessment of FMR severity plays a significant role even in mild MR. 3D VCA assessment in mild MR was described as problematic with low accuracy in previous studies [101, 104, 132] but we found it useful with reasonable reproducibility where the shape, size and length of VCA and number of jets could be assessed properly.

Our findings suggest that the presence of relatively large ellipsoid VCA at rest or multiple jets may be a marker of severe dynamic FMR despite the grading of FMR as “mild or moderate” by the recommended integrative approach. [3] In contrast, the small circular VCA characterizes stable mild to moderate FMR. In case of multiple jet current – guidelines do not allow to add widths of several VCs. Such attitude leads to underestimation in case of multiple jets and in our population would have affected 30% of patients. Thus, the colour Doppler 3D echocardiography-derived VCA allows direct assessment of ERO without geometric and flow assumptions, and hence, it is a promising new method for the quantification of FMR during exercise.

Apical rocking is a new marker to assess LV dyssynchrony and predict CRT response. [119] It is defined as an integrative surrogate of both temporal and functional inhomogeneities within the left ventricle which may be assessed visually with reasonable accuracy. [120, 121] We observed apical rocking more frequently in FMRi group (38% vs 6%, p=0,0018) and such findings was never described before.

Significantly more impaired function of the LV segment adjacent to the anterolateral PPM (akinetic or severely hypokinetic) was also significantly more often observed in FMRi group (46% vs 6%, p=0,0002).

When combined apical rocking and/or impaired anterolateral papillary muscle dysfunction showed accurate predictive values for FMRi with sensitivity 71%, specificity 87%, PPV 74%, NPV 85%. As we do know the presence of left ventricle dyssynchrony is a significant predictor of dynamic FMR as proven by Madaric et al. but well correctable by cardiac resynchronisation therapy (CRT).[53] Patients with severe dyssynchrony who received CRT after the stress testing were not included in our prognostic part of the study.

6.8.4. VCA at rest and clinical outcome

Previous studies have demonstrated that presence of resting FMR in patients after myocardial infarction or with ischemic LV dysfunction is associated with increased mortality,

increased admission rate for worsening heart failure and reduced functional capacity [6, 49, 61, 115]. In these studies, the cut-off value of ERO ≥ 20 mm², assessed using the 2D PISA or the pulsed Doppler volumetric methods, has identified individuals with the worst prognosis. Our study has included patients with mild to moderate FMR at rest assessed using the 2D integrative approach[45, 114]. In line with the inclusion criteria, in the current study, all patients had the PISA-derived ERO < 20 mm² at rest and the PISA-derived ERO has not predicted outcome. In contrast, the “prognostic” VCA ≥ 20 mm² at rest has been observed in 29% of study individuals and its presence has been associated with a significantly higher occurrence of composite endpoint.

Moreover, VCA ≥ 15 mm² has emerged as an independent predictor of outcome. Finally, a total of 26 (42%) patients showed large 3D VCL (≥ 7 mm) suggesting significant FMR at rest while no patients showed wide 2D vena contracta.

This suggests that the presence of relatively large ellipsoid VCA may be a marker of significant FMR with adverse outcome despite grading of FMR as “mild to moderate” using the 2D PISA or the vena contracta width method. This also suggests that the 2D-derived approach may underestimate severity of FMR in some patients. Currently, the 2D integrative method is the recommended approach to assess severity of FMR [45, 114]. This method integrates several 2D-based indices to circumvent limitations of each of these techniques. Recent studies have investigated the colour Doppler 3D echocardiography approach for FMR quantification by a direct measurement of ERO using VCA [79, 82, 101, 102, 133, 134]. VCA at rest has been shown to have higher correlation with the 2D integrative method or magnetic resonance-derived regurgitant volume than any single 2D method [102, 134]. In contrast, in patients with FMR, the PISA method significantly underestimated ERO by 27% due to the geometric and flow assumptions. The irregular hemielliptical shape of ERO is relatively common in FMR [135]. Asymmetric ERO leads to underestimation of FMR severity by commonly used 2D methods, such as PISA or vena contracta width [79, 82, 100-102, 133-135]. In contrast, the 3D technology used in the current study allows direct visualization of ERO with precise assessment of its area and longest diameter.

6.8.5. VCA during exercise and clinical outcome

Distinction of dynamic severe from stable mild FMR in patients with systolic LV dysfunction and mild to moderate FMR at rest is critical since the former being associated with reduced survival [6, 49, 59]. The landmark studies of Lancellotti showed wide range of exercise-induced changes in the PISA method- or pulsed Doppler volumetric method-derived ERO in patients with ischemic LV dysfunction [6]. The exercise-induced increase in the PISA-derived ERO ≥ 13 mm² has been associated with adverse outcome [6, 49].

Corroborating this finding, in the present study, patients with endpoint showed significantly larger VCA during exercise than patients without endpoint.

Moreover, the exercise-induced increased in VCA ≥ 20 mm² has been identified as an independent predictor of composite endpoint. In contrast to the previous studies, exercise-induced increase in the PISA ERO has not predicted the outcome.

The reasons may be several. In our study, only patients with mild to moderate FMR at rest have been included. In contrast, the study of Lancellotti enrolled also patients with higher degrees of FMR at rest [6, 49]. In the present study, both VCA and the PISA-derived ERO increased significantly, however, the rest to peak exercise differences of VCA were significantly larger than the differences of the PISA-derived ERO. Furthermore, the exercise-induced significant increase of the PISA-derived ERO (> 13 mm^2) identified only 10 out of 24 (58 %) of patients with significant increase in VCA (> 20 mm^2). The underestimation of ERO by the PISA method was observed predominantly in patients with severe distortion of the mitral valve geometry implying highly irregular ERO shape. Finally, the direct comparison of the VCA and the PISA-derived ERO is not possible, since the VCA reflects the anatomical surface of the regurgitant orifice, while the PISA-derived ERO represents the physiological parameter based on hydrodynamic theory of flow converging towards a restricted orifice. The limitation of a single 2D measurement in the setting of non-circular ERO may partly be compensated by using multiple 2D measurements in different echocardiography planes. However, this approach may substantially increase the data acquisition time, which may be of a crucial importance during exercise, when the time window to obtain images is limited. In contrast, a single recording in one echocardiography view is needed to acquire colour Doppler 3D dataset for the VCA assessment.

6.9. Limitations

1) In our study, a single-beat (live) 3D colour Doppler acquisition for the assessment of VCA has been used. The VCA assessment method is free of any flow or geometric assumptions compared to 2D PISA method. This is especially important in valves with non-circular and asymmetric regurgitant orifices such as in the functional MR and may lead to reclassification of the MR severity. [79, 82, 100, 101, 103, 104]

On the contrary, VCA assessment has several limitations. The limited spatial resolution of the reconstructed image poses a particular problem with small regurgitant orifice area but may not be as important in moderate to severe MR. [101, 104]

The most significant limitation of our study is limited spatial and temporal resolution for the measurement of 3D planimetry of vena contracta especially when using single beat acquisition mode with final FR 14 to 17.

The single-beat recording has relatively lower temporal resolution than the multiple-beat acquisition. In this study, the average number of frames per systole was between 6-8 at heart rates achieved. Supine bicycle exercise is associated with shortening of diastole and only minor changes in the duration of systole [122]. So, the HR achieved at peak exercise (average 100 bpm) has not been associated with the significant decrease in the number of frames per systole.

However, the single-beat compared to the multiple-beat acquisition has several distinct advantages in patients with heart failure undergoing exercise. These severely ill patients have often irregular heart rate due to atrial fibrillation or frequent premature beats. These individuals are not able to hold breath during exercise. Irregular heart rate and absence of apnoea lead to stitching and respiratory artefacts which hamper the accuracy of the multiple-beat-derived VCA during exercise. Therefore, in the present study, the single-beat data acquisition has been used with a patient serving as his own control between rest and exercise. In case we would have used recommended multi-beat acquisition we would have to exclude about one half of the patients already at rest due to irregularities in heart rate with further limitations as concerns dataset acquisition during exercise.

It could be interesting issue to further increase FR for single beat color Doppler acquisition for example using smaller volume sampling for only VCA. However, our result show reasonable acuuracy and reproducibility.

The choice of the systolic frame affects VCA measurement, depending on MR etiology[14, 107] resulting in interobserver variability.

Furthermore, 3D-VCA is easily affected by the multiplanar reformatting process used to obtain the cross-sectional plane for planimetry.

In patients with highly eccentric regurgitants jets or with long regurgitant orifices along the non-planar coaptation zone may non-orthogonal and single plane manner of cropping of the regurgitant jet lead to VCA overestimation.

The measurement can be also affected by colour bleeding into the grey scale image, resulting in overestimation of VCA. Therefore, calibration of results from various cropping planes with other severity data is necessary in each laboratory before this technique can be clinically applicable.

While this method is less time-consuming than other techniques, the post-processing still requires a significant time commitment (up to 2 minutes in experienced hands) and expertise.

Finally, the use of stitched 3D volumes predisposes to stitching artifact, which will affect the accuracy of the measurements. Although using nonstitched 3D acquisitions may help to overcome this problem, this technique is still often limited by temporal and spatial resolution.

2) Second significant limitation was arbitrary defininition of MR increase group where VCA rise by ≥0,2cm2 was considered as significant. It was empirically set up according to widely accepted prognostically important increase in ischemic MR ERO by ≥0,13cm2[6] We chose higher value for VCA change because of known trend for underestimation of true MR severity in FMR.

3) Third, functional capacity assessment was not measured directly by determining VO2max or VE/CO slope as recommended for heart failure patients, but was estimated from the highest cycle work rate achieved. Nevertheless we believe that significant difference in target work rate reflects lower functional capacity of FMRI group.

4) Fourth, as described in first chapter concerning, functional MR shows dynamic changes during systole typically with early and late systolic peaks and mid-systolic decrease. These changes reflects pressure revolution in LV and LA during systole with peak closing pressure in mid systole and are more pronounced in mild MR, however, 80% of regurgitant flow occurs in mid-systole.[15, 37]

We measured VCA and PISA radius at the same time during mid-systole to be able to compare these two methods. Tracking these dynamic changes of the ERO during the whole systole would be the most appropriate method, but unless fully automated, it is not usable in clinical medicine.

The most appropriate 3D colour Doppler method for the MR severity assessment was not established and currently is not recommended as a method of choice. Recent studies show promising results using methodics with 3D PISA assessment or volumetric analysis.[87, 110, 111] Further studies are needed to establish 3D echocardiography as routine method for MR severity assessment. Hopefully up-comming developement of new 3D systems will soon allow single beat dataset acquisition of bigger volumes and with better resolution as it is currently the most limiting factor for wide-spread use of 3D echocardiography.

6.10. Conclusion

We summarize our findings as follows:

Secondary:

1) We refuse our hypothesis that the relationship between exercise-induced changes of FMR assessed by VCA, clinical and Doppler characteristics is not different from those described by 2D-PISA methods previously.
2) We confirmed our hypothesis that there are resting predictors of exercise-induced changes in FMR assessed by VCA.
3) We confirmed our hypothesis that there is a difference between VCA and PISA methods for assessing FMR at rest and during exercise.

Primary:

4) We confirmed our hypothesis that VCA at rest and its increase during exercise is an independent predictor of clinical outcome in our population.

6.11. Author´s contribution to the study:

The whole study concept was set up during conversations with Dr. Martin Penicka at the beginning of my fellowship in echocardiography laboratory in Cardiovascular Centre in Aalst, Belgium. In year 2011 , the centre received a new high-end vendor enabling 3D colour Doppler echocardiography imaging, together with tilt-able bicycle ergometer providing the opportunity to run the study. At first, I have checked to feasibility and worked on the 3D image analysis work-up not only for the purpose of our study , but also for the other indications such as degenerative mitral valve regurgitation, septal defect flow quantification. I have been taught how to make and run database, provide statistical analysis of the data. I have personally provided the majority of echocardiography examinations, all the post-processing analysis and presented our results in many international meetings.

6.12. References

1. Nishimura, R.A., et al., *2014 AHA/ACC guideline for the management of patients with valvular heart disease: executive summary: a report of the American College of Cardiology/American Heart Association Task Force on Practice Guidelines.* J Am Coll Cardiol, 2014. **63**(22): p. 2438-88.
2. Vahanian, A., et al., *Guidelines on the management of valvular heart disease (version 2012): the Joint Task Force on the Management of Valvular Heart Disease of the European Society of Cardiology (ESC) and the European Association for Cardio-Thoracic Surgery (EACTS).* Eur J Cardiothorac Surg, 2012. **42**(4): p. S1-44.
3. Lancellotti, P., et al., *Recommendations for the echocardiographic assessment of native valvular regurgitation: an executive summary from the European Association of Cardiovascular Imaging.* Eur Heart J Cardiovasc Imaging, 2013. **14**(7): p. 611-44.

4. Fattouch, K., et al., *Papillary muscle relocation in conjunction with valve annuloplasty improve repair results in severe ischemic mitral regurgitation.* J Thorac Cardiovasc Surg, 2011. **143**(6): p. 1352-5.
5. Lancellotti, P., J.L. Zamorano, and M.A. Vannan, *Imaging challenges in secondary mitral regurgitation: unsolved issues and perspectives.* Circ Cardiovasc Imaging, 2014. **7**(4): p. 735-46.
6. Lancellotti, P., et al., *Prognostic importance of exercise-induced changes in mitral regurgitation in patients with chronic ischemic left ventricular dysfunction.* Circulation, 2003. **108**(14): p. 1713-7.
7. Bursi, F., et al., *Mitral regurgitation after myocardial infarction: a review.* Am J Med, 2006. **119**(2): p. 103-12.
8. Lamas, G.A., et al., *Clinical significance of mitral regurgitation after acute myocardial infarction. Survival and Ventricular Enlargement Investigators.* Circulation, 1997. **96**(3): p. 827-33.
9. Levine, R.A. and E. Schwammenthal, *Ischemic mitral regurgitation on the threshold of a solution: from paradoxes to unifying concepts.* Circulation, 2005. **112**(5): p. 745-58.
10. Trichon, B.H., et al., *Relation of frequency and severity of mitral regurgitation to survival among patients with left ventricular systolic dysfunction and heart failure.* Am J Cardiol, 2003. **91**(5): p. 538-43.
11. Magne, J., P. Lancellotti, and L.A. Pierard, *Exercise-induced changes in degenerative mitral regurgitation.* J Am Coll Cardiol, 2010. **56**(4): p. 300-9.
12. Tischler, M.D., et al., *Observations suggesting a high incidence of exercise-induced severe mitral regurgitation in patients with mild rheumatic mitral valve disease at rest.* J Am Coll Cardiol, 1995. **25**(1): p. 128-33.
13. Dal-Bianco, J.P., et al., *Basic mechanisms of mitral regurgitation.* Can J Cardiol, 2014. **30**(9): p. 971-81.
14. Hung, J., et al., *Mechanism of dynamic regurgitant orifice area variation in functional mitral regurgitation: physiologic insights from the proximal flow convergence technique.* J Am Coll Cardiol, 1999. **33**(2): p. 538-45.
15. Schwammenthal, E., et al., *Dynamics of mitral regurgitant flow and orifice area. Physiologic application of the proximal flow convergence method: clinical data and experimental testing.* Circulation, 1994. **90**(1): p. 307-22.
16. He, S., et al., *Integrated mechanism for functional mitral regurgitation: leaflet restriction versus coapting force: in vitro studies.* Circulation, 1997. **96**(6): p. 1826-34.
17. Kono, T., et al., *Left ventricular shape is the primary determinant of functional mitral regurgitation in heart failure.* J Am Coll Cardiol, 1992. **20**(7): p. 1594-8.
18. Otsuji, Y., et al., *Insights from three-dimensional echocardiography into the mechanism of functional mitral regurgitation: direct in vivo demonstration of altered leaflet tethering geometry.* Circulation, 1997. **96**(6): p. 1999-2008.
19. Kalra, K., et al., *Temporal changes in interpapillary muscle dynamics as an active indicator of mitral valve and left ventricular interaction in ischemic mitral regurgitation.* J Am Coll Cardiol, 2014. **64**(18): p. 1867-79.
20. Liang, Y.J., et al., *Incremental value of global systolic dyssynchrony in determining the occurrence of functional mitral regurgitation in patients with left ventricular systolic dysfunction.* Eur Heart J, 2012. **34**(10): p. 767-74.
21. Gertz, Z.M., et al., *Evidence of atrial functional mitral regurgitation due to atrial fibrillation: reversal with arrhythmia control.* J Am Coll Cardiol, 2011. **58**(14): p. 1474-81.
22. Takahashi, Y., et al., *Mitral valve repair for atrial functional mitral regurgitation in patients with chronic atrial fibrillation.* Interact Cardiovasc Thorac Surg, 2015. **21**(2): p. 163-8.
23. Beaudoin, J., et al., *Mitral valve enlargement in chronic aortic regurgitation as a compensatory mechanism to prevent functional mitral regurgitation in the dilated left ventricle.* J Am Coll Cardiol, 2013. **61**(17): p. 1809-16.

24. Timek, T.A., et al., *Mitral leaflet remodeling in dilated cardiomyopathy.* Circulation, 2006. **114**(1 Suppl): p. I518-23.
25. Laughlin, M.H., *Cardiovascular response to exercise.* Am J Physiol, 1999. **277**(6 Pt 2): p. S244-59.
26. Manou-Stathopoulou, V., et al., *The effects of cold and exercise on the cardiovascular system.* Heart, 2015. **101**(10): p. 808-20.
27. Slutsky, R., et al., *Response of left ventricular volume to exercise in man assessed by radionuclide equilibrium angiography.* Circulation, 1979. **60**(3): p. 565-71.
28. Crawford, M.H., M.A. Petru, and C. Rabinowitz, *Effect of isotonic exercise training on left ventricular volume during upright exercise.* Circulation, 1985. **72**(6): p. 1237-43.
29. Furukawa, K., et al., *Left ventricular size and performance during graded supine exercise in normal subjects.* Jpn Heart J, 1983. **24**(4): p. 503-14.
30. La Gerche, A., et al., *Cardiac MRI: a new gold standard for ventricular volume quantification during high-intensity exercise.* Circ Cardiovasc Imaging, 2012. **6**(2): p. 329-38.
31. Paulsen, W.J., et al., *Ventricular response to isometric and isotonic exercise. Echocardiographic assessment.* Br Heart J, 1979. **42**(5): p. 521-7.
32. Lewis, G.D., et al., *Pulmonary vascular hemodynamic response to exercise in cardiopulmonary diseases.* Circulation, 2013. **128**(13): p. 1470-9.
33. Naeije, R., et al., *Exercise-induced pulmonary hypertension: physiological basis and methodological concerns.* Am J Respir Crit Care Med, 2013. **187**(6): p. 576-83.
34. Bossone, E., et al., *Range of tricuspid regurgitation velocity at rest and during exercise in normal adult men: implications for the diagnosis of pulmonary hypertension.* J Am Coll Cardiol, 1999. **33**(6): p. 1662-6.
35. Lebrun, F., P. Lancellotti, and L.A. Pierard, *Quantitation of functional mitral regurgitation during bicycle exercise in patients with heart failure.* J Am Coll Cardiol, 2001. **38**(6): p. 1685-92.
36. Heinle, S.K., F.D. Tice, and J. Kisslo, *Effect of dobutamine stress echocardiography on mitral regurgitation.* J Am Coll Cardiol, 1995. **25**(1): p. 122-7.
37. Keren, G., et al., *Dynamic mitral regurgitation. An important determinant of the hemodynamic response to load alterations and inotropic therapy in severe heart failure.* Circulation, 1989. **80**(2): p. 306-13.
38. Shen, W.F., et al., *Left ventricular volume and ejection fraction response to exercise in chronic congestive heart failure: difference between dilated cardiomyopathy and previous myocardial infarction.* Am J Cardiol, 1985. **55**(8): p. 1027-31.
39. Tomai, F., et al., *Left ventricular volumes during exercise in normal subjects and patients with dilated cardiomyopathy assessed by first-pass radionuclide angiography.* Am J Cardiol, 1993. **72**(15): p. 1167-71.
40. Keren, G., et al., *Effect of isometric exercise on cardiac performance and mitral regurgitation in patients with severe congestive heart failure.* Am Heart J, 1989. **118**(5 Pt 1): p. 973-9.
41. Mann, D.L., et al., *Left ventricular volume during supine exercise: importance of myocardial scar in patients with coronary heart disease.* J Am Coll Cardiol, 1987. **9**(1): p. 26-34.
42. Ennezat, P.V., et al., *Myocardial asynchronism is a determinant of changes in functional mitral regurgitation severity during dynamic exercise in patients with chronic heart failure due to severe left ventricular systolic dysfunction.* Eur Heart J, 2006. **27**(6): p. 679-83.
43. Giga, V., et al., *Exercise-induced changes in mitral regurgitation in patients with prior myocardial infarction and left ventricular dysfunction: relation to mitral deformation and left ventricular function and shape.* Eur Heart J, 2005. **26**(18): p. 1860-5.
44. Izumo, M., et al., *Three-dimensional echocardiographic assessments of exercise-induced changes in left ventricular shape and dyssynchrony in patients with dynamic functional mitral regurgitation.* Eur J Echocardiogr, 2009. **10**(8): p. 961-7.

45. Lancellotti, P., F. Lebrun, and L.A. Pierard, *Determinants of exercise-induced changes in mitral regurgitation in patients with coronary artery disease and left ventricular dysfunction.* J Am Coll Cardiol, 2003. **42**(11): p. 1921-8.
46. Lancellotti, P., et al., *Effect of dynamic left ventricular dyssynchrony on dynamic mitral regurgitation in patients with heart failure due to coronary artery disease.* Am J Cardiol, 2005. **96**(9): p. 1304-7.
47. Lapu-Bula, R., et al., *Contribution of exercise-induced mitral regurgitation to exercise stroke volume and exercise capacity in patients with left ventricular systolic dysfunction.* Circulation, 2002. **106**(11): p. 1342-8.
48. Takano, H., et al., *Functional mitral regurgitation during exercise in patients with heart failure.* Circ J, 2006. **70**(12): p. 1563-7.
49. Lancellotti, P., P.L. Gerard, and L.A. Pierard, *Long-term outcome of patients with heart failure and dynamic functional mitral regurgitation.* Eur Heart J, 2005. **26**(15): p. 1528-32.
50. Bertrand, P.B., et al., *Exercise Dynamics in Secondary Mitral Regurgitation: Pathophysiology and Therapeutic Implications.* Circulation, 2017. **135**(3): p. 297-314.
51. Peteiro, J., et al., *The effect of exercise on ischemic mitral regurgitation.* Chest, 1998. **114**(4): p. 1075-82.
52. Schwammenthal, E. and R.A. Levine, *The non-ischaemic dynamics of ischaemic mitral regurgitation: solving the paradox.* Eur Heart J, 2005. **26**(15): p. 1454-5.
53. Madaric, J., et al., *Early and late effects of cardiac resynchronization therapy on exercise-induced mitral regurgitation: relationship with left ventricular dyssynchrony, remodelling and cardiopulmonary performance.* Eur Heart J, 2007. **28**(17): p. 2134-41.
54. Rossi, A., et al., *Independent prognostic value of functional mitral regurgitation in patients with heart failure. A quantitative analysis of 1256 patients with ischaemic and non-ischaemic dilated cardiomyopathy.* Heart, 2011. **97**(20): p. 1675-80.
55. Szymanski, C., et al., *Impact of mitral regurgitation on exercise capacity and clinical outcomes in patients with ischemic left ventricular dysfunction.* Am J Cardiol, 2011. **108**(12): p. 1714-20.
56. Yamano, T., et al., *Exercise-induced changes of functional mitral regurgitation in asymptomatic or mildly symptomatic patients with idiopathic dilated cardiomyopathy.* Am J Cardiol, 2008. **102**(4): p. 481-5.
57. Lancellotti, P., et al., *Clinical significance of exercise pulmonary hypertension in secondary mitral regurgitation.* Am J Cardiol, 2015. **115**(10): p. 1454-61.
58. Claessen, G., et al., *Accuracy of Echocardiography to Evaluate Pulmonary Vascular and RV Function During Exercise.* JACC Cardiovasc Imaging, 2015. **9**(5): p. 532-43.
59. Pierard, L.A. and P. Lancellotti, *The role of ischemic mitral regurgitation in the pathogenesis of acute pulmonary edema.* N Engl J Med, 2004. **351**(16): p. 1627-34.
60. Baumgartner, H., et al., *2017 ESC/EACTS Guidelines for the management of valvular heart disease.* Eur Heart J, 2017. **38**(36): p. 2739-2791.
61. Grigioni, F., et al., *Ischemic mitral regurgitation: long-term outcome and prognostic implications with quantitative Doppler assessment.* Circulation, 2001. **103**(13): p. 1759-64.
62. Ponikowski, P., et al., *2016 ESC Guidelines for the diagnosis and treatment of acute and chronic heart failure: The Task Force for the diagnosis and treatment of acute and chronic heart failure of the European Society of Cardiology (ESC)Developed with the special contribution of the Heart Failure Association (HFA) of the ESC.* Eur Heart J, 2016. **37**(27): p. 2129-2200.
63. Cleland, J.G., et al., *The effect of cardiac resynchronization on morbidity and mortality in heart failure.* N Engl J Med, 2005. **352**(15): p. 1539-49.
64. Breithardt, O.A., et al., *Acute effects of cardiac resynchronization therapy on functional mitral regurgitation in advanced systolic heart failure.* J Am Coll Cardiol, 2003. **41**(5): p. 765-70.
65. Ypenburg, C., et al., *Mechanism of improvement in mitral regurgitation after cardiac resynchronization therapy.* Eur Heart J, 2008. **29**(6): p. 757-65.

66. Ypenburg, C., et al., *Acute effects of initiation and withdrawal of cardiac resynchronization therapy on papillary muscle dyssynchrony and mitral regurgitation.* J Am Coll Cardiol, 2007. **50**(21): p. 2071-7.
67. Penicka, M., et al., *Predictors of improvement of unrepaired moderate ischemic mitral regurgitation in patients undergoing elective isolated coronary artery bypass graft surgery.* Circulation, 2009. **120**(15): p. 1474-81.
68. Fattouch, K., et al., *POINT: Efficacy of adding mitral valve restrictive annuloplasty to coronary artery bypass grafting in patients with moderate ischemic mitral valve regurgitation: a randomized trial.* J Thorac Cardiovasc Surg, 2009. **138**(2): p. 278-85.
69. Chan, K.M., et al., *Coronary artery bypass surgery with or without mitral valve annuloplasty in moderate functional ischemic mitral regurgitation: final results of the Randomized Ischemic Mitral Evaluation (RIME) trial.* Circulation, 2012. **126**(21): p. 2502-10.
70. Smith, P.K., et al., *Surgical treatment of moderate ischemic mitral regurgitation.* N Engl J Med, 2014. **371**(23): p. 2178-88.
71. Bertrand, P.B., et al., *Mitral valve area during exercise after restrictive mitral valve annuloplasty: importance of diastolic anterior leaflet tethering.* J Am Coll Cardiol, 2015. **65**(5): p. 452-61.
72. Fino, C., et al., *Restrictive mitral valve annuloplasty versus mitral valve replacement for functional ischemic mitral regurgitation: an exercise echocardiographic study.* J Thorac Cardiovasc Surg, 2013. **148**(2): p. 447-53 e2.
73. Grayburn, P.A., et al., *Relationship between the magnitude of reduction in mitral regurgitation severity and left ventricular and left atrial reverse remodeling after MitraClip therapy.* Circulation, 2013. **128**(15): p. 1667-74.
74. Zoghbi, W.A., et al., *Recommendations for Noninvasive Evaluation of Native Valvular Regurgitation: A Report from the American Society of Echocardiography Developed in Collaboration with the Society for Cardiovascular Magnetic Resonance.* J Am Soc Echocardiogr, 2017. **30**(4): p. 303-371.
75. Chen, C.G., et al., *Impact of impinging wall jet on color Doppler quantification of mitral regurgitation.* Circulation, 1991. **84**(2): p. 712-20.
76. Zoghbi, W.A., et al., *Recommendations for evaluation of the severity of native valvular regurgitation with two-dimensional and Doppler echocardiography.* J Am Soc Echocardiogr, 2003. **16**(7): p. 777-802.
77. Hall, S.A., et al., *Assessment of mitral regurgitation severity by Doppler color flow mapping of the vena contracta.* Circulation, 1997. **95**(3): p. 636-42.
78. Matsumura, Y., et al., *Geometry of the proximal isovelocity surface area in mitral regurgitation by 3-dimensional color Doppler echocardiography: difference between functional mitral regurgitation and prolapse regurgitation.* Am Heart J, 2008. **155**(2): p. 231-8.
79. Yosefy, C., et al., *Direct measurement of vena contracta area by real-time 3-dimensional echocardiography for assessing severity of mitral regurgitation.* Am J Cardiol, 2009. **104**(7): p. 978-83.
80. Enriquez-Sarano, M., et al., *Effective mitral regurgitant orifice area: clinical use and pitfalls of the proximal isovelocity surface area method.* J Am Coll Cardiol, 1995. **25**(3): p. 703-9.
81. Schwammenthal, E., et al., *Mechanism of mitral regurgitation in inferior wall acute myocardial infarction.* Am J Cardiol, 2002. **90**(3): p. 306-9.
82. Iwakura, K., et al., *Comparison of orifice area by transthoracic three-dimensional Doppler echocardiography versus proximal isovelocity surface area (PISA) method for assessment of mitral regurgitation.* Am J Cardiol, 2006. **97**(11): p. 1630-7.
83. Biner, S., et al., *Reproducibility of proximal isovelocity surface area, vena contracta, and regurgitant jet area for assessment of mitral regurgitation severity.* JACC Cardiovasc Imaging, 2010. **3**(3): p. 235-43.

84. Bargiggia, G.S., et al., *A new method for quantitation of mitral regurgitation based on color flow Doppler imaging of flow convergence proximal to regurgitant orifice.* Circulation, 1991. **84**(4): p. 1481-9.
85. Quaini, A., et al., *A Three-Dimensional Computational Fluid Dynamics Model of Regurgitant Mitral Valve Flow: Validation Against in vitro Standards and 3D Color Doppler Methods.* Cardiovasc Eng Technol, 2012. **2**(2): p. 77-89.
86. Li, X., et al., *Flow convergence flow rates from 3-dimensional reconstruction of color Doppler flow maps for computing transvalvular regurgitant flows without geometric assumptions: An in vitro quantitative flow study.* J Am Soc Echocardiogr, 1999. **12**(12): p. 1035-44.
87. Little, S.H., et al., *In vitro validation of real-time three-dimensional color Doppler echocardiography for direct measurement of proximal isovelocity surface area in mitral regurgitation.* Am J Cardiol, 2007. **99**(10): p. 1440-7.
88. Sitges, M., et al., *Real-time three-dimensional color doppler evaluation of the flow convergence zone for quantification of mitral regurgitation: Validation experimental animal study and initial clinical experience.* J Am Soc Echocardiogr, 2003. **16**(1): p. 38-45.
89. Buck, T. and B. Plicht, *Real-Time Three-Dimensional Echocardiographic Assessment of Severity of Mitral Regurgitation Using Proximal Isovelocity Surface Area and Vena Contracta Area Method. Lessons We Learned and Clinical Implications.* Curr Cardiovasc Imaging Rep, 2015. **8**(10): p. 38.
90. Lang, R.M., et al., *EAE/ASE recommendations for image acquisition and display using three-dimensional echocardiography.* Eur Heart J Cardiovasc Imaging, 2012. **13**(1): p. 1-46.
91. Hung, J., et al., *3D echocardiography: a review of the current status and future directions.* J Am Soc Echocardiogr, 2007. **20**(3): p. 213-33.
92. Rankin, R.N., et al., *Three-dimensional sonographic reconstruction: techniques and diagnostic applications.* AJR Am J Roentgenol, 1993. **161**(4): p. 695-702.
93. Pandian, N.G., et al., *Dynamic three-dimensional echocardiography: methods and clinical potential.* Echocardiography, 1994. **11**(3): p. 237-59.
94. Cheng, T.O., et al., *Real-time 3-dimensional echocardiography in assessing atrial and ventricular septal defects: an echocardiographic-surgical correlative study.* Am Heart J, 2004. **148**(6): p. 1091-5.
95. Zamorano, J., et al., *Real-time three-dimensional echocardiography for rheumatic mitral valve stenosis evaluation: an accurate and novel approach.* J Am Coll Cardiol, 2004. **43**(11): p. 2091-6.
96. Badano, L.P., et al., *High volume-rate three-dimensional stress echocardiography to assess inducible myocardial ischemia: a feasibility study.* J Am Soc Echocardiogr, 2010. **23**(6): p. 628-35.
97. Little, S.H., *The vena contracta area: conquering quantification with a 3D cut?* JACC Cardiovasc Imaging, 2012. **5**(7): p. 677-80.
98. Khanna, D., et al., *Quantification of mitral regurgitation by live three-dimensional transthoracic echocardiographic measurements of vena contracta area.* Echocardiography, 2004. **21**(8): p. 737-43.
99. Yosefy, C., et al., *Proximal flow convergence region as assessed by real-time 3-dimensional echocardiography: challenging the hemispheric assumption.* J Am Soc Echocardiogr, 2007. **20**(4): p. 389-96.
100. Kahlert, P., et al., *Direct assessment of size and shape of noncircular vena contracta area in functional versus organic mitral regurgitation using real-time three-dimensional echocardiography.* J Am Soc Echocardiogr, 2008. **21**(8): p. 912-21.
101. Little, S.H., et al., *Three-dimensional color Doppler echocardiography for direct measurement of vena contracta area in mitral regurgitation: in vitro validation and clinical experience.* JACC Cardiovasc Imaging, 2008. **1**(6): p. 695-704.

102. Marsan, N.A., et al., *Quantification of functional mitral regurgitation by real-time 3D echocardiography: comparison with 3D velocity-encoded cardiac magnetic resonance.* JACC Cardiovasc Imaging, 2009. **2**(11): p. 1245-52.
103. Shanks, M., et al., *Quantitative assessment of mitral regurgitation: comparison between three-dimensional transesophageal echocardiography and magnetic resonance imaging.* Circ Cardiovasc Imaging, 2010. **3**(6): p. 694-700.
104. Zeng, X., et al., *Diagnostic value of vena contracta area in the quantification of mitral regurgitation severity by color Doppler 3D echocardiography.* Circ Cardiovasc Imaging, 2011. **4**(5): p. 506-13.
105. Hyodo, E., et al., *Direct measurement of multiple vena contracta areas for assessing the severity of mitral regurgitation using 3D TEE.* JACC Cardiovasc Imaging, 2012. **5**(7): p. 669-76.
106. Yoganathan, A.P., et al., *Review of hydrodynamic principles for the cardiologist: applications to the study of blood flow and jets by imaging techniques.* J Am Coll Cardiol, 1988. **12**(5): p. 1344-53.
107. Buck, T., et al., *Effect of dynamic flow rate and orifice area on mitral regurgitant stroke volume quantification using the proximal isovelocity surface area method.* J Am Coll Cardiol, 2008. **52**(9): p. 767-78.
108. Plicht, B., et al., *Direct quantification of mitral regurgitant flow volume by real-time three-dimensional echocardiography using dealiasing of color Doppler flow at the vena contracta.* J Am Soc Echocardiogr, 2008. **21**(12): p. 1337-46.
109. Grady, L., et al., *Regurgitation quantification using 3D PISA in volume echocardiography.* Med Image Comput Comput Assist Interv, 2011. **14**(Pt 3): p. 512-9.
110. de Agustin, J.A., et al., *Direct measurement of proximal isovelocity surface area by single-beat three-dimensional color Doppler echocardiography in mitral regurgitation: a validation study.* J Am Soc Echocardiogr, 2012. **25**(8): p. 815-23.
111. Thavendiranathan, P., et al., *Quantification of chronic functional mitral regurgitation by automated 3-dimensional peak and integrated proximal isovelocity surface area and stroke volume techniques using real-time 3-dimensional volume color Doppler echocardiography: in vitro and clinical validation.* Circ Cardiovasc Imaging, 2012. **6**(1): p. 125-33.
112. Choi, J., et al., *Differential effect of 3-dimensional color Doppler echocardiography for the quantification of mitral regurgitation according to the severity and characteristics.* Circ Cardiovasc Imaging, 2014. **7**(3): p. 535-44.
113. Schmidt, F.P., et al., *Usefulness of 3D-PISA as compared to guideline endorsed parameters for mitral regurgitation quantification.* Int J Cardiovasc Imaging, 2014. **30**(8): p. 1501-8.
114. Boyd, J.H., *Ischemic mitral regurgitation.* Circ J, 2013. **77**(8): p. 1952-6.
115. Grigioni, F., et al., *Contribution of ischemic mitral regurgitation to congestive heart failure after myocardial infarction.* J Am Coll Cardiol, 2005. **45**(2): p. 260-7.
116. Ennezat, P.V., et al., *Exercise does not enhance the prognostic value of Doppler echocardiography in patients with left ventricular systolic dysfunction and functional mitral regurgitation at rest.* Am Heart J, 2008. **155**(4): p. 752-7.
117. Lancellotti, P., et al., *Recommendations for the echocardiographic assessment of native valvular regurgitation: an executive summary from the European Association of Cardiovascular Imaging.* Eur Heart J Cardiovasc Imaging. **14**(7): p. 611-44.
118. Lang, R.M., et al., *Recommendations for chamber quantification.* Eur J Echocardiogr, 2006. **7**(2): p. 79-108.
119. Stankovic, I., et al., *Relationship of visually assessed apical rocking and septal flash to response and long-term survival following cardiac resynchronization therapy (PREDICT-CRT).* Eur Heart J Cardiovasc Imaging, 2015. **17**(3): p. 262-9.
120. Szulik, M., et al., *Assessment of apical rocking: a new, integrative approach for selection of candidates for cardiac resynchronization therapy.* Eur J Echocardiogr, 2010. **11**(10): p. 863-9.

121. Tournoux, F., et al., *Absence of left ventricular apical rocking and atrial-ventricular dyssynchrony predicts non-response to cardiac resynchronization therapy.* Eur Heart J Cardiovasc Imaging, 2012. **13**(1): p. 86-94.

122. Chung, C.S., M. Karamanoglu, and S.J. Kovacs, *Duration of diastole and its phases as a function of heart rate during supine bicycle exercise.* Am J Physiol Heart Circ Physiol, 2004. **287**(5): p. H2003-8.

123. Izumo, M., et al., *Changes in mitral regurgitation and left ventricular geometry during exercise affect exercise capacity in patients with systolic heart failure.* Eur J Echocardiogr, 2011. **12**(1): p. 54-60.

124. Sutton, T.M., et al., *Plasma natriuretic peptide levels increase with symptoms and severity of mitral regurgitation.* J Am Coll Cardiol, 2003. **41**(12): p. 2280-7.

125. Lancellotti, P., B. Cosyns, and L.A. Pierard, *Dynamic left ventricular dyssynchrony contributes to B-type natriuretic peptide release during exercise in patients with systolic heart failure.* Europace, 2008. **10**(4): p. 496-501.

126. D'Andrea, A., et al., *Effect of dynamic myocardial dyssynchrony on mitral regurgitation during supine bicycle exercise stress echocardiography in patients with idiopathic dilated cardiomyopathy and 'narrow' QRS.* Eur Heart J, 2007. **28**(8): p. 1004-11.

127. Lafitte, S., et al., *Dynamic ventricular dyssynchrony: an exercise-echocardiography study.* J Am Coll Cardiol, 2006. **47**(11): p. 2253-9.

128. Lin, B.A., et al., *Color Doppler jet area overestimates regurgitant volume when multiple jets are present.* J Am Soc Echocardiogr, 2010. **23**(9): p. 993-1000.

129. Izumo, M., et al., *Changes in mitral regurgitation and left ventricular geometry during exercise affect exercise capacity in patients with systolic heart failure.* Eur J Echocardiogr, 2010. **12**(1): p. 54-60.

130. Enriquez-Sarano, M., et al., *Quantitative determinants of the outcome of asymptomatic mitral regurgitation.* N Engl J Med, 2005. **352**(9): p. 875-83.

131. Penicka, M., et al., *Prognostic Implications of Magnetic Resonance-Derived Quantification in Asymptomatic Patients With Organic Mitral Regurgitation: Comparison With Doppler Echocardiography-Derived Integrative Approach.* Circulation, 2017. **137**(13): p. 1349-1360.

132. Skaug, T.R., et al., *Quantification of mitral regurgitation using high pulse repetition frequency three-dimensional color Doppler.* J Am Soc Echocardiogr, 2009. **23**(1): p. 1-8.

133. Shanks, M., et al., *Quantitative assessment of mitral regurgitation: comparison between three-dimensional transesophageal echocardiography and magnetic resonance imaging.* Circ Cardiovasc Imaging.2010, **3**(6): p. 694-700.

134. Zeng, X., et al., *Diagnostic value of vena contracta area in the quantification of mitral regurgitation severity by color Doppler 3D echocardiography.* Circ Cardiovasc Imaging. 2011, **4**(5): p. 506-13.

135. Grayburn, P.A., N.J. Weissman, and J.L. Zamorano, *Quantitation of mitral regurgitation.* Circulation. 2012, **126**(16): p. 2005-17.